frontiers in Built Environment

TYPE Original Research
PUBLISHED 23 March 2026
DOI 10.3389/fbuil.2026.1768439

OPEN ACCESS

EDITED BY
Benedetta Moccia,
Sapienza University of Rome, Italy

REVIEWED BY
Herban Sorin,
Politehnica University of Timişoara, Romania
Fereshteh Taromideh,
Università della Campania Luigi Vanvitelli, Italy

*CORRESPONDENCE
Stavroula Sigourou,
s.sigourou@gmail.com

RECEIVED 15 December 2025
REVISED 12 February 2026
ACCEPTED 13 February 2026
PUBLISHED 23 March 2026

CITATION
Sigourou S, Dimitriadis P, Pagana V, Tsouni A, Iliopoulou T, Sargentis G-F, Ioannidis R, Dimitrakopoulou D, Chardavellas E, Mamassis N, Koutsoyiannis D and Kontoes CH (2026) Developing an integrated methodology for flood-hazard assessment: application to the Pikrodafni River Basin (Attica, Greece).
Front. Built Environ. 12:1768439.
doi: 10.3389/fbuil.2026.1768439

Developing an integrated methodology for flood-hazard assessment: application to the Pikrodafni River Basin (Attica, Greece)

Stavroula Sigourou[1]*, Panayiotis Dimitriadis[2], Vasiliki Pagana[1], Alexia Tsouni[1,3], Theano Iliopoulou[2], G.-Fivos Sargentis[2], Romanos Ioannidis[4], Dimitra Dimitrakopoulou[2], Efthymios Chardavellas[2], Nikos Mamassis[2], Demetris Koutsoyiannis[2] and Charalampos (Haris) Kontoes[1]

[1]Operational Unit "BEYOND Centre of EO Research & Satellite Remote Sensing", Institute for Astronomy, Astrophysics, Space Applications and Remote Sensing (IAASARS), National Observatory of Athens (NOA), Athens, Greece, [2]Laboratory of Hydrology and Water Resources Development, School of Civil Engineering, National Technical University of Athens, Athens, Greece, [3]Edge in Earth Observation Sciences, Athens, Greece, [4]Department of Architecture, Built Environment and Construction Engineering, Politecnico di Milano, Milan, Italy

Flood hazard assessment—together with vulnerability and risk analysis—is closely linked to flood resilience and has been extensively studied in densely populated areas, where the most catastrophic floods tend to occur. The need for a holistic and transferable methodology is critical considering that, different simulation approaches are often used, while key methodological phases are sometimes omitted. Within the framework of the Programming Agreement of the Prefecture of Attica, the BEYOND Centre (IAASARS/NOA), in cooperation with the NTUA research group have developed the methodology presented in this work. The methodology was implemented at high spatial resolution in five flood-affected river basins in Attica, with the Pikrodafni River basin being presented in detail in this study. Data acquisition constituted a core component of the methodology and involved targeted spatial datasets, Earth-observation imagery, time-series data, historical flood records, and relevant prior studies obtained from the competent authorities. Field visits were conducted to characterize site conditions and verify the collected datasets, identifying high-risk critical points, and measuring the dimensions of hydraulic structures (bridges, culverts) and channel properties. Regarding modeling, design-flood scenarios with typical return periods were analyzed in accordance with the Directive 2007/60/EC. HEC-HMS was used to generate hydrographs for each sub-basin, which were then imported into the quasi-2D LISFLOOD-FP model as a means to prepare and calibrate the HEC-RAS model, where a rain-on-grid methodology integrated the hydrologic and hydraulic flood processes at the area of interest. High spatial resolution was maintained throughout, with particular emphasis on uncertainty analysis and on the detailed representation of infrastructure and urban areas, given their strong influence on flood dynamics. Results indicate that overflow typically occurs in buried streams, along adjacent roads in the downstream reach of the river, at

stream confluences, and at the upstream inlet where natural streams enter the drainage pipe network. Up to 200 critical points were identified, of which up to 35% were classified as first-priority sites for intervention.

KEYWORDS

field surveys, flood hazard assessment framework, hydraulic dynamics, rainfall-runoff model, urban river management

1 Introduction

Natural hazards constitute a major global threat, with floods ranking among the most frequent and damaging events affecting both human systems and the natural environment. In 2024, floods remained one of the most impactful natural hazards worldwide (Centre for Research on the Epidemiology of Disasters, 2025), while flash floods are particularly destructive in the Mediterranean region (Diakakis et al., 2019). Flood-related mortality highlights the severity of these hazards and underscores the need for systematic flood-risk assessment that explicitly addresses short-duration extremes and urban exposure. This need is already well established within European and national policy frameworks.

Urban expansion has significantly amplified flood risk. Historically, cities avoided natural floodplains; however, rapid and largely uncontrolled urban growth increasingly encroached upon them without adequate flood-protection planning. As a result, extensive flood-defense infrastructure and river channelization became necessary to sustain urban functionality (Sargentis et al., 2025b). Such measures are typically designed for return periods of 25–50 years, leaving cities highly vulnerable to more extreme hydrological events.

In recent years, the European Union has prioritized pluvial flooding driven by short-duration, high-intensity rainfall, recognizing that its impacts often extend across entire catchments rather than being confined to river corridors (Ennouini et al., 2024). Compound pluvial–fluvial flooding, which can be more severe than either process alone, further intensifies flood impacts (Guan et al., 2023). These processes emphasize the necessity for advanced rainfall modeling and improved assessment of hydrometeorological impacts (Varra et al., 2025).

Flood risk is commonly defined as the combination of hazard, exposure, and vulnerability (Van Westen, 2013; Wannous and Velasquez, 2017). Flood-risk assessment approaches range from empirical and statistical methods to multi-criteria and index-based frameworks, which offer efficient tools for preliminary evaluations (de Moel et al., 2009; Merz et al., 2010; Kourgialas and Karatzas, 2013). Hazard assessment often relies on hydrodynamic modeling, with physically based models providing detailed representations of terrain, land cover, and hydraulic structures, albeit at the cost of increased data and computational demands (Rozos et al., 2023).

Hyper-resolution two-dimensional inundation models are increasingly applied for flood-hazard mapping (Wing et al., 2024). The open-source LISFLOOD-FP model is widely used in Copernicus services such as the European Flood Awareness System (Zábori et al., 2024), often coupled with rainfall–runoff models such as HEC-HMS (Sargentis et al., 2025c). Similarly, the Rain-on-Grid methodology implemented in HEC-RAS enables simulation of pluvial and compound flooding using spatially distributed rainfall inputs from gauges, radar, satellites, and numerical forecasts (Ennouini et al., 2024; U.S. Army Corps of Engineers, Hydrologic Engineering Center, 2025). Continuous model development and calibration remain essential to improve accuracy and reduce uncertainty (Dimitriadis et al., 2016).

Urban areas particularly vulnerable to flooding due to high population density, asset concentration, impervious surfaces, and engineered drainage networks (European Parliament Council of the European Union, 2007; Loukas, 2015; Wang et al., 2023; Yan et al., 2024). Urbanization increases runoff coefficients, shortens hydrological response times, and intensifies short-duration rainfall extremes, thereby elevating flood risk (Yan et al., 2024). Consequently, accurate identification of flood-prone urban areas is critical for effective risk assessment, planning, and resilience-building (Zhou et al., 2025).

Within this context, flood-risk reduction has become a priority under international and European frameworks, including the Sendai Framework for Disaster Risk Reduction 2015–2030 and the EU Floods Directive 2007/60/EC (European Parliament Council of the European Union, 2007; United Nations Office for Disaster Risk Reduction, 2015). In Greece, strategic flood-risk mitigation is essential for compliance with these directives and national water-management policies (Koutsoyiannis et al., 2008; Diakakis et al., 2019).

This study presents a flood-hazard assessment methodology applied to the Pikrodafni urban river basin in Attica in 2021. Pikrodafni is one of the few remaining open streams in the region, despite ongoing discussions regarding its resectioning or partial covering. The disappearance and culverting of urban streams have been widespread practices in Greece, often increasing flood risk (Koutsoyiannis et al., 2012). Nature-based solutions are increasingly proposed as alternatives to conventional grey infrastructure, offering flood-risk reduction alongside ecological and aesthetic benefits (Ourloglou et al., 2020).

Attica is characterized by extensive urbanization, high population density, critical infrastructure, and recurring flood events, despite relatively low average annual rainfall (Koutsoyiannis and Baloutsos, 2000; Hellenic Statistical Authority, 2021). Wildfires, floodplain narrowing, and widespread stream burial further exacerbate flood risk (Wyżga et al., 2018; Partington et al., 2022).

Within this framework, a Programming Agreement signed in March 2021 between the Region of Attica and NOA initiated a comprehensive assessment of earthquake, fire, and flood risks. The methodology introduced integrates hazard, vulnerability, and exposure analyses to identify critical flood-prone areas and propose mitigation measures across several high-risk river basins, including Pikrodafni (Tsouni et al., 2025).

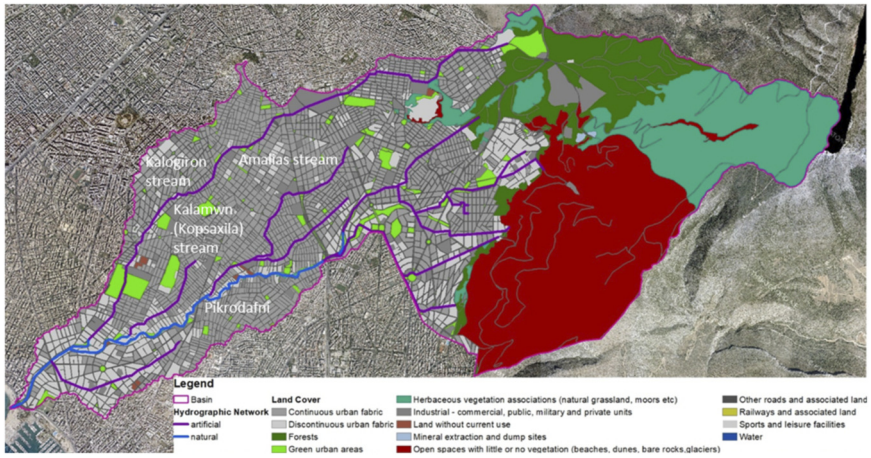

FIGURE 1
Land use/land cover of pikrodafni river basin.

2 Materials and methods

2.1 Study area

The study area is the Pikrodafni River basin in the Water Department of Attica, a region officially designated as flood-prone under national and EU assessments. Part of the river basin is characterized as Areas of Potentially Significant Flood Risk according to the first Revision of the Preliminary Flood Risk Assessment (Ministry of Environment and Energy, 2023) and is exposed to flooding according to the Flood Risk Management Plan for Attica (Ministry of Environment and Energy, 2025). Both documentations constitute deliverables required by the EU Floods Directive (2007/60/EC) (European Parliament Council of the European Union, 2007), as implemented in Greece for Attica River Basin Districts (EL-06) and provide a robust basis for the selection of the study area as a representative case of high flood hazard and management challenges.

The Pikrodafni basin lies in southeastern Attica and traverses a densely urbanized landscape. This urbanization is reflected in both population and land cover. The most relevant municipalities host ~41.7k–78.2k residents each (dominant ages 40–49 in Alimos, Palaio Faliro, Ilioupoli and 30–39 in Agios Dimitrios) (Hellenic Statistical Authority, 2021). Land-cover data, obtained by 2018 Urban Atlas database from Copernicus Land Monitoring Service (European Environment Agency, 2021), show urban fabric 36.33%, herbaceous vegetation 12.93%, forest 7.44%, burned areas 19.81% (2015 & 2020), and road network 14.01%, a composition indicative of high imperviousness and wildfire impact that can increase peak runoff. Specifically, two significant wildfire events, from 2015 to 2020, were integrated into the LULC dataset to capture their lasting impacts. The stream rises on the western slopes of Mount Hymettus and discharges into Phaleron Bay near Alimos Marina ("EDEM"). A notable recent flood event occurred on 22 February 2013, with most damages concentrated near the estuary. The basin covers 24.99 km^2 (perimeter 30.94 km) and is oriented northeast–southwest. Most of its river network is artificial except for the downstream part of Pikrodafni river (Figure 1). It spans the municipalities of Palaio Faliro, Alimos, Agios Dimitrios, Nea Smyrni, Ilioupoli, Vyronas, Dafni-Ymittos, and Kaisariani. Elevations range from 0 m to 1,023.45 m (mean ≈267 m); steep slopes dominate the upstream, mountainous sector on Hymettus, while the lowland reach extends from Vouliagmenis Avenue to the outflow.

The climate is Mediterranean, with dry, hot summers and mild winters (Anagnostopoulos and Co, 2018). Records from the Nymphs' Hill (Thissio, Athens) meteorological station for 1983–2012 time period indicate an average annual precipitation of ~400 mm and mean monthly temperatures from 10.2 °C in January to 29.1 °C in July.

2.2 Data collection

For the successful implementation of this study, different types of data were collected to ensure a comprehensive understanding of all relevant parameters. These data serve multiple purposes, including the analysis of key variables and the development of accurate models.

The collected datasets cover a wide range of aspects, including spatial data, data gathered from field visits, and data from technical studies. The spatial data required for the study comprise comprehensive Earth observation datasets, ensuring a detailed and accurate representation of the study area. Specifically, the land use/land cover (LULC) (Figure 1) dataset is derived from the European Urban Atlas, produced under the Copernicus program. To enhance the accuracy of the LULC dataset, burnt areas were integrated using data from the Burnt Scar Mapping (BSM) service of the "FireHUB" system, developed by the Operational Unit BEYOND Centre IAASARS/NOA. Updating the land-cover layer to include burned areas is essential, given their significant impact on surface runoff, hydrological modeling, and consequently flood hazard assessment (Kyriakouli, 2022). Additionally, the spatial dataset of the Curve Number, utilized to enhance hydrological modeling and provided by the Ministry of the Environment and Energy, was also updated with the burnt areas. Moreover, a 2 m spatial resolution Digital Elevation Model (DEM),

derived by large scale orthoimagery LSO25 for the period 2014-2016, is used (Stathakis, 2022). This dataset serves as a fundamental component for the detailed and hydrological and hydraulic analyses, facilitating accurate terrain representation, watershed delineation, and flood modeling. Finally, data from Open Street Map (OSM), such as the road network, is utilized and integrated in the HEC-RAS model to enforce terrain discontinuities and improve the representation of the flow.

Complementary, in order to achieve a more comprehensive flood risk assessment for the region, data were collected both from past studies and from relevant public authorities. These datasets were systematically processed and integrated into a modern GIS-based framework, including textual descriptions, CAD drawings, and GIS files. Each data type requires careful pre-processing to resolve issues such as scale, format, and coordinate systems. The validity of older infrastructure (e.g., culverts, bridges, channel linings, embankments) and terrain information was assessed against current conditions, with targeted field verification and by addressing clarifications from the responsible authorities and implementing both backward checks to the source and forward on-site checks. Input from experienced staff at the authorities was incorporated to confirm interpretations and fill out missing attributes. All data were checked, completed, and organized to ensure the production of reliable datasets for robust hydrological and hydraulic modeling and flood risk assessment.

2.3 Field surveys

Throughout this work, the combination of engineering studies and on-site inspection was identified as an integral component of a comprehensive approach to infrastructure assessment and management (Mattas et al., 2023; Sigourou et al., 2023). Therefore, detailed field visits in the examined riverbed and the broader region, were implemented, and were combined with the utilization of modern mapping tools, including Google Earth, digital terrain models, satellite imagery and online geolocation services. Conventional methods for contact with local communities were also implemented, such as questionnaires for surveying public perceptions of flood hazards and relevant infrastructure works (Residents, 2025) and free-format interviews with locals.

The questionnaire was forwarded to groups in social media and acquaintances, so that it would be filled by randomly selected people in the Attica Region. The filling of the questionnaire was preferred to be anonymous, and people were asked beforehand whether their replies can be used for the research; two choices that facilitated even more the procedure. We believe that due to all the above reasons, a lot of data was finally acquired. People working in institutes were also asked to participate in this research by filling in the questionnaire. The experience of the latter is highly appreciated, since they usually occupy an academic position in engineering schools, which enables them to approach this study in a more technical manner.

With the aim to identify areas prone to high flood-risk, a direct contact through brief interviews with the public in each area was attempted during the in-site visits along the streams and rivers in the areas of interest, to ensure the viability of the responses. Particularly, besides the filling of the questionnaire, people were asked for their opinion on any past flooding incidents or upon specific locations prone to high-frequency flooding. Notably, people showed reluctance during the in-site filling of the questionnaires. Only a small percentage of the questionnaire was filled during in-site visits, since in most cases, people seemed to be skeptical when approached by scientists and asked questions related to flood-risk and possible future mitigation work.

Residents possess intimate knowledge of their neighborhoods, including drainage patterns, flood-prone areas, and past flood events. In particular, their contribution is important due to the identification of vulnerable areas, prioritizing projects, sense of ownership, proposing effective solutions for each area, maintaining the infrastructure, and spreading awareness.

Specialized engineering teams were organized, prepared, and split into groups of two to cover the broader area of the riverbeds, in areas with walking access.

A clearly developed methodology was implemented for field visits in the presented work in the streams of Attica Region, Greece including Pikrodafni river. This structured methodology ensured a comprehensive and systematic approach to on-site inspections, enabling accurate assessment of site conditions, proper documentation of critical infrastructure elements, and effective post-event analysis (Sigourou et al., 2022b; Sigourou et al., 2022a). It consisted of the following three primary steps.

A. Pre-Inspection Preparation

Prior to fieldwork, a structured pre-processing phase was conducted to identify and document critical observation points within the study area. The desktop screening involved utilizing Google Earth Pro and satellite images to analyze hydrographic networks and integrating data from various sources (e.g., master plans, flood monitoring observatories, national statistics and national databases) in order to identify the critical points as a first step for clarification during field research and further enhance them with extras points. Following the analysis of satellite imagery and digital terrain models, engineers identified critical points, which are associated with the behavior of the riverbeds during flood events. To clarify those critical points, to locate them and analyze during field research, in order to verify the accuracy of the collected data.

Before accessing them on-site, these critical points were supplemented with information derived from satellite imagery and historical studies. A standardized coding of the critical points was used in the marking of critical points, so that the engineer in the field would know what they would expect to see. Each critical point was marked with a pin that initially included: (a) The stream branch, e.g., R1.1; (b) The ascending pin number; e.g., P1; (c) The type of the needed observation and measures: e.g., G = Bridge, C = Culvert, O = Confluence of a stormwater pipe into a stream, D = Critical cross-section, K=Changes in riverbed, B=Buildings; (d) the critical point's characteristics such as the shape and the dimensions. The standardized coding was presented in Table 1.

Critical points were marked with georeferenced pins following the previously mentioned standardized coding system and arranged sequentially from downstream to upstream. After that, .kmz files

TABLE 1 Standardized protocol for coding of the critical points in field surveys.

Stream branch	Ascending pin number	Type of point & information sources	Characteristics
R1.1	P1	G = Bridge 	• Construction material MAT (e.g., Concrete = b, Iron = f, Wood = w) • Bridge shape and dimensions DIM • Channel bed material MANb and left bank MAN l (in the direction of flow) and right bank MANr (in the direction of flow) (e.g., Soil = p, Vegetation = f, Stones = s, Reinforced concrete = b)
		C = culvert (below channel bed) or channel widening Opening area >1 m^2 or Ø120 cm 	• Shape and dimensions of the culvert along the channel DIM
		O = Outfall of stormwater pipe into stream 	• Shape and dimensions of stormwater outlet DIM
		K = Change in channel cross-section (either widening or narrowing) 	• Shape and dimensions of the channel cross-section in regulated river sections DIM • Channel bed material MANb and banks MANl (left) and MANr (right) (in the direction of flow) (Soil = p, Vegetation = f, Stones = s, Reinforced concrete = b) note: In compound channels, two width values will be recorded
		D = channel bank failure or collapse 	• Irish crossing IRI • Loose or eroded riverbanks, risk of slope failure/landslide PRA • Constructions within the streambeds and stream slopes (likely illegal) CON • Trees with exposed root systems that may be uprooted and carried downstream TRE • Garbage and construction debris likely to block drainage systems and culverts BAZ

were exported, containing the marked points, which were distributed to different fieldwork teams for site inspection assigned to predefined regions.

Before the fieldwork teams accessed the field, navigation tools were installed in the smart phones of the team members to facilitate access to the maps of the critical points and offline map services (MAPS.ME and Google Earth in particular). During the field work, additional critical points could also be identified and incorporated into the dataset.

B. Field Inspection Execution

The inspections followed a predefined methodology, which defined what the engineers expected to see, what needed to be measured, how to measure it, and potential issues they could encounter.

Initially, on the field, coordinated organization of the working teams was required to ensure that the inspections would be conducted safely, always during daylight hours, in groups of at

least two engineers and within a specific duration (up to 8 h in the field per day, to prevent accidents due to fatigue or haste). Additionally, for site inspections in floodplains, rivers, and streams, it was initially necessary to plan visits during periods of minimal water flow and to monitor weather bulletins to protect the teams from the possibility of sudden flood events. It was important to ensure that the engineers in the field would not be exposed to any danger. In this regard, it was clarified to the teams to pay attention to the stability of the slopes when approaching the bed without risking their physical integrity under any circumstances. Emergency contact numbers were also available, and attention was given to communication methods to support the social acceptance of the engineers in the field, to ensure that no conflicts would arise (especially in the parts of the riverbed where it was possible that locals disapproved of detailed recording of their properties by public institutions). The primary method in this regard was description of the nature of the research with honesty and description of its intent and social-scientific contribution.

During on-site inspections, teams followed a systematic approach to collect and document spatial and structural data: (i) Enabling GPS tracking on mobile devices for precise geolocation; (ii) Using Google Earth and MAPS.ME to navigate through predefined observation points; (iii) The team would visit the critical point, capture photos, make the necessary measurements and observations, and immediately afterward recorded a short video in which they verbally stated the name of the critical point and then their observations and measurements, while also capturing the point in video. Since the engineers have all necessary information on their mobile devices, the absence of notebooks and writing materials was very helpful and increased the flexibility of movement and associated safety (iv) Recording unexpected findings such as unregistered drainage systems, constructions within the streambeds and stream slopes (likely illegal), or new structural vulnerabilities. When additional critical points emerged in the field (e.g., evidence of erosion, flood damage, or infrastructure instability), new pins were added in MAPS.ME. These additional pins were labeled with an intermediate numbering system (e.g., R1.2–P3a-C) and visually distinguished from pre-processed markers for verification at a later stage.

C. Data Processing and Integration

Upon returning from the field, all collected data was systematically processed to ensure consistency and accuracy. This included (i) Immediately transferring photographs and videos from mobile devices to a shared Google Photos folder designated for each inspection day, (ii) integrating additional pins created in MAPS.ME into the master.kmz file in Google Earth, (ii) linking photographic records to their corresponding georeferenced points in Google Earth using URL-based image embedding, (iv) and reviewing collected video footage to extract key site characteristics and updating the descriptive metadata of each observation point (measurements, roughness of the riverbeds, etc.). Finally, the deliverables were detailed technical reports for each critical point containing the code name, representative photos and detailed description, as presented in Figure 9 of the Results.

This repeatable, safety-aware, and data-rich protocol integrated multi-source desktop analysis with targeted field verification, producing decision-ready evidence for infrastructure assessment and flood-risk management of the study area of the Pikrodafni stream.

2.4 Design rainfall estimation

To derive the design rainfall intensity (x) for a certain timescale (k) and return period (T), we employed the design rainfall curves of the study area for 50, 100, 1000 years return periods according to the EU Flood Directive (European Parliament Council of the European Union, 2007). To this aim, we used the design rainfall curves developed by Iliopoulou and Koutsoyiannis (Iliopoulou and Koutsoyiannis, 2022) using rainfall data from local meteorological stations, and following the general methodology introduced by Koutsoyiannis et al. (Koutsoyiannis et al., 2024). Accordingly, the relationship between the rainfall intensity x (e.g., mm/h) for time scale k (e.g., h) and return period T (e.g., years) was given by:

$$x = \lambda \frac{\left(T/\beta\right)^{\xi} - 1}{\left(1 + k/\alpha\right)^{\eta}}, \xi > 0$$

where λ is an intensity scale parameter in units of rainfall intensity (here, mm/h), α is a timescale parameter in units of timescale (here, h), η is a dimensionless persistence parameter, ξ > 0 is a dimensionless parameter representing the upper tail-index of the process, and β is a scale parameter for the return period in units of return period (here, years).

For the Pikrodafni basin, α (h), η (−), ξ (−) and β (years) were estimated using a spatial pooling methodology for the Attica region, equal to, 0.1 h, 0.73, 0.07, and 0.07 years, while the scale parameter λ (mm/h) was estimated based on the spatial distribution of elevation in the Pikrodafni basin, equal to 489.22 mm/h (Iliopoulou and Koutsoyiannis, 2022). This yielded a total rainfall depth for 24 h equal to 108.64 mm, 123.29 mm, 177.39 mm, for 50, 100 and 1000 years return period, respectively.

We note that a recent regionalization of the design rainfall relationships provided these parameters at a grid of 5 km × 5 km covering the entire Greek territory, thus eliminating the need for performing regional estimations for each study area (Iliopoulou et al., 2024).

For assigning a temporal distribution to the design rainfall event (hyetograph), we employed the established Alternating Block method (Chow et al., 1988). For a chosen storm duration and temporal resolution, cumulative rainfall depths for successive durations were first obtained from the design rainfall relationships for each return period, and the corresponding incremental (partial) block depths were derived by differencing consecutive cumulative values. The resulting blocks were then ranked in descending order, with the largest placed at the midpoint of the total duration and the remaining blocks arranged alternately to the left and right of the central one. The Alternating Block Method was used because it provided a simple, reproducible, and physically reasonable way to distribute the total design rainfall depth over time, producing hyetographs that reflect realistic storm structures while preserving the prescribed total depth. The hyetograph duration was set to 24 h, exceeding the basin's time of concentration in order to ensure that the full runoff response and

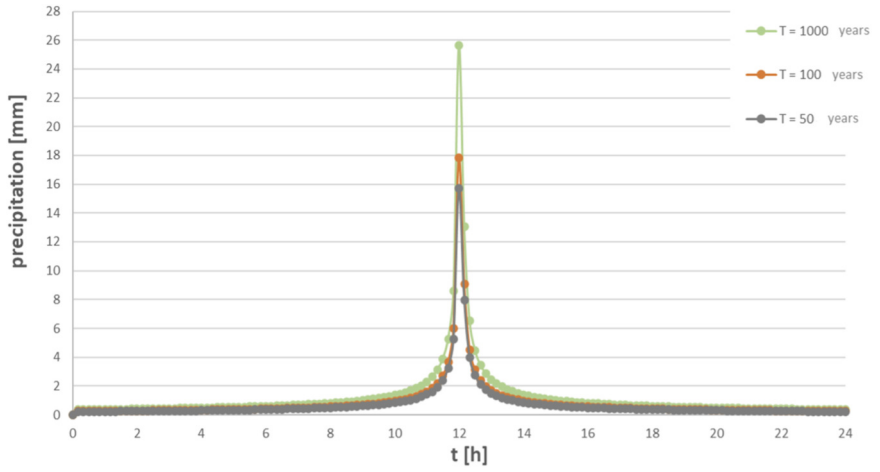

FIGURE 2
Design hyetographs for Pikrodafni river basin for 50, 100 and 1000-year return period.

the peak discharge at the outlet were captured in all scenarios. This conservative choice is appropriate for flood-hazard assessment and does not imply uniform rainfall intensity throughout the event, as short-duration extremes are incorporated through the rainfall intensity-timescale-return period relationships and the Alternating Block Method. The selected temporal resolution of the hyetograph (10 min), commonly used in hydrological simulations of flood events—particularly for small catchments—further ensures that high-intensity sub-hour rainfall peaks are adequately represented.

The point rainfall intensities obtained from the design rainfall relationships were converted to areal rainfall intensities by multiplying them by the surface reduction coefficient φ (Koutsoyiannis and Xanthopoulos, 1999), given by the following equation.

$$\varphi = \max\left\{1 - \frac{0.048A^{0.36-0.01\ln A}}{d^{0.35}}, 0.25\right\}$$

where A is the catchment area in km^2 and k is the time scale in hours. It should be noted that the coefficient φ was applied both to the total rainfall depth corresponding to the overall duration of the design storm, and to the sectional rainfall depths corresponding to each individual time scale within the hyetograph.

Overall, applying the aforementioned equations, the design hyetographs of 24-h rainfall were derived for the entire drainage basin for return periods of 50, 100, and 1000 years, which are depicted in the following chart in grey, orange, and green color, respectively (Figure 2).

Differences are observed between the hyetographs, with the most significant ones found at the peak (12 h of rainfall), where the values reach 15.7 mm, 17.8 mm, and 25.6 mm for the three return periods, respectively.

2.5 Hydrologic analysis and modeling

The type of flood needs to be clarified in order to decide the approach in modeling and in flood hazard assessment, respectively. The fact that the Pikrodafni river basin is highly urbanized can lead to increased surface runoff and exacerbate pluvial flooding during storm events. Together with the fluvial flooding, compound pluvial-fluvial flooding can lead to more severe impacts and thus needs to be simulated, respectively.

The hydrological analysis of the basin needs to be preceded by hydrologic modeling. Runoff estimation was performed using the open-access software HEC-HMS (Hydrologic Engineering Center–Hydrologic Modeling System) (U.S. Army Corps of Engineers, Hydrologic Engineering Center, 2018), developed by the U.S. Army Corps of Engineers. The software was designed to comprehensively simulate hydrological processes in dendritic drainage basins. Flow hydrographs derived by rainfall-runoff model will be imported to LISFLOOD-FP model, as explained in the corresponding section.

Subbasins were delineated according to the hydrographic network and major land-cover differences. When a subbasin includes a transition from rural to urban land cover, it was further subdivided to better represent the land cover changes. Land use/land cover parameter is considered as a key factor in rainfall-runoff simulation having significant impact on runoff (Sajikumar and Remya, 2015). Thus, increased accuracy of the hydrologic model should be achieved by designing catchments with similar characteristics.

The river basin was divided into 40 subbasins, as presented in the following Figure, covering almost 25 km^2 area. The geometry of the hydrologic basin including the substreams and the subbasins was imported in the rainfall-runoff model with the form of a schematic diagram (Figure 3).

Regarding the hydrologic analysis procedures, the selected methods were based on the application of i) the Soil Conservation Service's Runoff Curve Number and ii) the SCS Unit Hydrograph.

i. The SCS-CN (Soil Conservation Service (SCS), 1972) was implemented for the estimation of precipitation excess (maximum precipitation excess he [mm]) for the separation

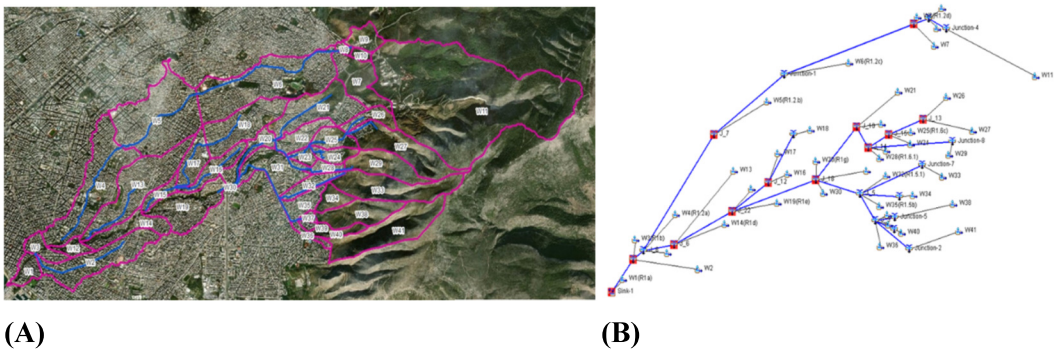

(A) (B)

FIGURE 3
(A) Sub-basins of Pikrodafni river basin. **(B)** Schematic of river basin in HEC-HMS.

of hydrological losses from the total hyetograph according to the following empirical equations.

$$h_e = \begin{cases} 0 & h \le 0.2S \\ \dfrac{(h-0.2S)^2}{h+0,8S} & h > 0.2S \end{cases}$$

$$S = 254\left(\frac{100}{CN} - 1\right)$$

where, S: maximum potential retention [mm]

CN: Curve Number CN.

The hydrologic analysis was conducted for dry (CN I), average (CN II) and wet (CN III) antecedent soil moisture conditions. The values for the average antecedent soil moisture conditions (type II, CN II) were provided in polygon format by the Department of Flood and Drought Risk Management & Demand Management of the General Directorate for Water of the Ministry of Environment and Energy. The area - weighted average CN value was estimated for each subbasin by running a built-up workflow in Model Builder application in GIS. Next, the dry (CN I) and the wet (CN III) antecedent soil moisture conditions were also estimated regarding the reference values of average antecedent soil moisture conditions (CN II) according to the equations below.

$$CN_I = \frac{0.42\,CN_{II}}{1 - 0.0058CN_{II}}$$

$$CN_{III} = \frac{2.3\,CN_{II}}{1 + 0.013CN_{II}}$$

ii. Regarding the Synthetic Unit Hydrograph (SUH) method, SCS method (Soil Conservation Service (Soil Conservation Service (SCS), 1972) was chosen for transforming the precipitation excess into runoff (hydrograph), where lag time (t_L) needs to be imported. Specifically, the spatiotemporal transformation of the contributed precipitation excess into runoff (design flood hydrographs) was achieved by implementing the SUI method (Koukouvinos, 2014).

For each subbasin, lag time was assessed regarding the time of concentration t_c. Lag time represents the time between the center of mass of the effective rainfall hyetograph and the center of mass of the direct runoff hydrograph (time of peak of discharge).

$$t_L = 0.6t_c$$

where tc: time of concentration of the basin [min]

The time of concentration was estimated by applying two empirical equations, Giandotti and Kirpich formulas. The Giandotti formula is generally well applied to the Greek territory according to Tsakiri (Loukas, 2015), for plain hydrological basins with natural deformed riverbed, as established within the Presidential Decree 696/1974 of the Hellenic Republic (Presidential Decree, 1974). Also, Giandotti formula is considered to assess more accurately the time of concentration in large basins with high surface runoff and collected runoff water inside the watercourse (Region of Thessaly, 2020). Therefore, for the aforementioned reasons, Giandotti method was chosen to be applied for the upstream rural subbasins of the study area (Giandotti, 1934).

$$t_c = \frac{4\sqrt{A} + 1.5L}{0.8\sqrt{\Delta z}}$$

where A: area of the basin [km^2]

L: length of the main watercourse [km]

Δz: Difference in elevation between the average elevation of the basin and the elevation of the outlet [m]

On the other hand, Kirpich formula (Kirpich, 1940) is suggested to be applied in small rural river basins covering from 0.003 to 0.5 km^2. Also, together with the fact that the time of concentration is overestimated using Giandotti formula, Kirpich method was considered as the most suitable for the small urban river basins of the study area.

$$t_c = 0.0667L^{0.77}/S^{0.385}$$

where L: length of the main watercourse [km]

S: average slope [m/m]

Apart from the rainfall-runoff model, the SCS method was also used in the hydraulic model HEC-RAS to account for hydrologic losses from the total hyetograph and to calculate the direct rainfall, which was uniformly distributed across the basin area and converted

into runoff. A detailed description of this process is provided in the corresponding chapter.

In HEC-HMS, the meteorological model was developed for each scenario, assigning each subbasin a design hyetograph derived from ombrian curves for a 24-h rainfall event corresponding to return periods of 50, 100 and 1000 years. All design hyetographs (timeseries) were organized and stored using the HEC-DSS (Hydrologic Engineering Center - Data Storage System) software. Additionally, the average antecedent soil moisture conditions (CN II) were chosen as the most representative conditions for Pikrodafni's river basin, thus three scenarios were created according to the chosen return periods.

2.6 Hydraulic modeling

For the hydraulic analysis and flood inundation maps, HEC-RAS 6.0 (Hydrologic Engineering Center (CEIWR-HEC) River Analysis System) (U.S. Army Corps of Engineers, 2020) and LISFLOOD-FP (Bates and De Roo, 2000) software were chosen to be utilized for modeling of the river basin of Pikrodafni river. The accurate but computationally demanding 2D HEC-RAS model was prepared and calibrated based on the results of the quasi-2D LISFLOOD-FP model, which exhibits significantly lower computational costs. Generally, the 2D hydraulic simulation provides greater flexibility in modeling diverse hydraulic scenarios, including urban and riverine flooding as well as hydraulic structure adaptations, making it ideal for various applications, alternative solutions, and improved resilience planning (Siakara et al., 2024). The main advantage of a 2D model is that it allows water to flow in a different direction, and the grid creates a denser network for the representation of the ground surface (Mattas et al., 2023).

The use of multiple flood simulation models, each employing a different mathematical solution approach aims to constrain the inherent uncertainties of the flood process and improve the reliability of key outputs (such as flow velocity and depth).

The selection of these particular hydraulic models was primarily driven by LISFLOOD-FP's quasi-2D nature, which allows for faster simulations. Specifically, running multiple simulations with different combinations of hydraulic parameters has proven valuable for identifying isolated flood-prone areas that typically form outside the main river channel; areas that might not be detected when relying on a single parameter combination. Examples of hydraulic parameters with high inherent uncertainty include local topographic slope (Cook and Merwade, 2009) and Manning's roughness coefficient (Manning, 1891) for both the main channel and the floodplain (Pappenberger et al., 2005; Papaioannou et al., 2017). These uncertainties may arise due to factors such as sediment erosion or deposition. Additionally, uncertainties stem from how buildings are represented in the hydraulic model (Bellos and Tsakiris, 2015), the resolution of computational grid cells, and the temporal step of the numerical solution scheme (Dimitriadis et al., 2016).

To conclude, the computationally intensive HEC-RAS 2D, which can solve the full 2D Saint-Venant equations (Chow, 1959) was calibrated based on LISFLOOD-FP results and was expected to improve the accuracy of flood inundation simulations.

2.6.1 LISFLOOD-FP

LISFLOOD-FP is a quasi-2d, raster-based model appropriate for various flow conditions. Its main advantage is that it allows using a high-resolution grid-based topographic terrain, and can process up to 10^6 grid cells, thus, being suitable for implementing probabilistic investigations based on Monte Carlo approaches. The main limitation is that it considers only rectangular channel cross-sections, which makes it more suitable for large basins with wide and shallow channels. The diffusive wave scheme was used for lateral floodplain inundation, where the 1d channel and floodplain routings were linked via a quasi, two-dimensional continuity equation (Bates et al., 2013).

The model setup for the Pikrodafni stream and its wider surrounding area involved the development of the following input files: (a) stream csv containing coordinate data, elevation, Manning roughness coefficients, and rectangular channel widths; (b) DEM providing elevations for all grid cells expected to be affected by flood inundation; (c) corresponding DEM assigning Manning roughness coefficients for the same grid cell resolution used in the elevation DEM; (d) boundary conditions, specifying the hydraulic conditions at the limits of the computational domain (typically using a kinematic wave boundary condition); (e) inflow hydrographs imposed at the stream channel or over the broader floodplain; and (f) control file, listing the names of the aforementioned inputs as well as the produced file for storing the simulated depth and velocity outputs.

The simulations conducted covered hydraulic conditions associated with return periods of 50, 100, and 1000 years; computational grid resolutions of 20 m, 10 m, and 5.6 m across the extended floodplain; and two channel-modification scenarios, one representing excavation (favorable scenario) and the other embankment (unfavorable scenario), implemented to ensure a negative longitudinal slope along the channel. The latter configuration was required for solving the kinematic wave in the main channel, as opposed to the dynamic wave, which can be solved even under positive slopes but incurs substantially higher computational costs. With the kinematic-wave approach, computational time was reduced to approximately 3.5 h for a 5.6 m grid, 1.0 h for a 10 m grid, and 0.5 h for a 20 m grid. Conversely, dynamic-wave simulations were rejected due to excessive computational demands, exceeding 1 day of processing time. For all scenarios, the computational time step was set to the automatic mode, allowing it to vary adaptively to satisfy the Courant stability criterion. The LISFLOOD model was first calibrated and validated using qualitative and semi-quantitative approaches. The calibration of key parameters such as Manning's roughness coefficient was based on field observations and the validation of the results based on reported past flood events (e.g., from questionnaires) at the area of interest.

2.6.2 HEC-RAS

HEC-RAS 6.0 version (Hydrologic Engineering Center's (CEIWR-HEC) River Analysis System) (U.S. Army Corps of Engineers, 2020) is an open-source software designed by the US Army Corps of Engineers. From all the provided types of

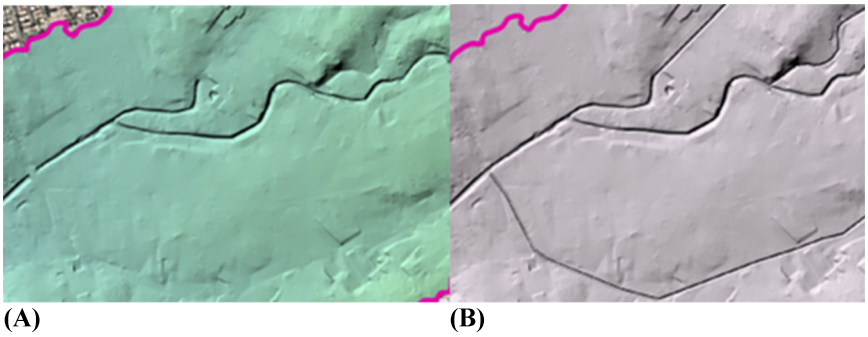

FIGURE 4
(A) Pre-modification DEM representation **(B)** and Post-modification DEM representation in the downstream area of Pikrodafni river basin.

simulations, HEC-RAS was used to perform two-dimensional unsteady flow calculations.

2D rain-on-grid (RoG) methodologies or direct rainfall methods can be particularly beneficial for pluvial and compound fluvial and pluvial floods (Ennouini et al., 2024), since the rainfall was applied spatially and temporarily distributed over the river basin, represented as a 2-dimensional domain. The RoG method constitutes a novel implementation that spatially distributes rainfall over the study area and integrates hydrological loss estimation directly into HEC-RAS.

Thus, hyetographs for each return period were imported as boundary conditions without pre-subtracting losses, which were estimated internally using the SCS Curve Number method to derive effective rainfall (precipitation excess). Accordingly, the downstream channel slope was specified via the normal-depth condition.

At first, terrain was created using a modified DEM of 2 m spatial resolution and following a two-dimensional mesh of varied spatial resolution – 2D Flow Area - was produced containing the simulation area. Additionally, roads, river banks and streamline were imported as Break Lines from shapefiles in order to align the mesh faces along. Manning values were inserted into the model as well by associating each land cover type with its corresponding Manning value for the study area.

A 2-m spatial resolution Digital Elevation Model from Greek Cadastre was used as terrain and was analytically checked and locally modified by properly incorporating the river network into the DEM in order to enforce the flow. Specifically, the main river network was modeled comprehensively, including both open and buried stream sections, in order to achieve high simulation accuracy. For the open segments of the hydrographic network, the terrain was appropriately modified in locations where the riverbed was poorly represented. Conversely, buried stream segments were represented as open channels rather than as culverts, since explicitly importing a large number of culverts into HEC-RAS was impractical due to the complexity of the high-resolution computational mesh and the need to also incorporate stormwater grates within the model. Geometric characteristics of the riverbeds, culverted streams, and hydraulic structures (e.g., bridges) were derived from field surveys and relevant technical studies. The following Figure illustrates the incorporation of two critical buried tributaries into the terrain within the downstream confluence area of the river basin (Figure 4).

In addition, two new spatial information layers were created: the polygons of land cover (land cover layer) and the polygons of the Curve Number (CN II) under average antecedent soil moisture conditions for calculating hydrological losses due to infiltration (infiltration layer). For each CORINE land cover class, a Manning roughness coefficient value corresponded according to the specifications of the Flood Risk Management Plans under the Floods Directive 2007/60/EC (European Parliament Council of the European Union, 2007). Consequently, the land cover classes from Urban Atlas were matched with the corresponding CORINE Land Cover classes, so that the Manning coefficient value can be assigned subsequently.

There are various methods that simulate the influence of buildings on flood inundation (Bellos and Tsakiris, 2015; Beretta et al., 2018). In this study, increased roughness coefficient was applied in land cover classes corresponding to buildings (11100, 11200, and 11300), effectively representing their impact on flooding at the building block level.

With regard to initial losses, their percentage may vary depending on the storm event and the type of catchment (Woodward et al., 2003). In this study, the following assumption was adopted: for Curve Number values below 77, the initial losses are set at 20%, representing agricultural and forest areas, while for values above 77, the initial losses are assumed to be 5%, a value commonly applied for urban areas, as reported by Liam et al. (Patel, 2009). In the post-fire areas (CN > 77), the assumption is that the initial losses are set to 5% for safety reasons. The land cover and infiltration layers, together with the terrain, were associated with the generated geometry.

The creation of the geometry of the model is essential. The basin geometry consists of a two-dimensional mesh, slightly expanded beyond the watershed boundary, which serves as the computational grid for the hydraulic simulation. The mesh spatial resolution varies with areas of interest. A base cell size of 25 m was used over most of the domain, whereas higher resolution is applied near the channel. The stream centerlines were encoded as 2d breaklines, with local refinement around these lines to cell sizes of 1–10 m and 3–10 m, in order to better resolve channel hydraulics and enhance numerical accuracy. Additionally, a mesh refinement region (refinement tool) was defined, encompassing a 100 m buffer zone on both sides of the channel along its entire length, with a target cell size of 5–10 m.

The HEC-RAS 2D model has a new type of numerical scheme that permits efficiencies, whereby a relatively coarse numerical grid can be used (e.g., 10 m), for which the sub grid topography (2 m) is taken into account. This is achieved through precomputing

hydraulic tables for each coarse numerical grid cell, comprising the conveyance across each face as a function of sub grid geometry, and then also a table of storage volume in the cell as a function of water elevation. This permits the modeling of channels that pass through the numerical cells if they are represented in the sub grid topography (Hankin et al., 2019).

Numerous trials were performed to stabilize the model geometry and determine the optimal spatial resolution, given the large extent of the catchment and the model's capabilities. Therefore, an automated procedure was developed to reduce the time of creating the model's geometry, which is transferable and applicable to any study areas.

To generate the computational mesh, a novel workflow was implemented in which a two-dimensional grid with enforced breaklines is precomputed within a database management system (DBMS). At each step, cells that violate HEC-RAS geometric constraints are analytically identified and flagged. Using this theoretically optimal grid as a template, a sequence of automated HEC-RAS routines is executed—without manual intervention—in an iterative loop until convergence to an error-free mesh suitable for simulation. The algorithm is implemented in Python and leverages a spatially enabled PostgreSQL/PostGIS database.

The simulation horizon was selected to capture the system response at peak flooding—the stage at which flood-hazard maps were derived. Accordingly, the total duration was set to the time required for the flood wave to reach its peak at the basin outlet, augmented by a safety factor. Thus, hydraulic simulations were performed for 28 h using a variable time step of 0.1 s. The set of equations used for simulations were the two-dimensional Saint–Venant equations (Shallow Water Equations, Eulerian method SWE-EM). To accommodate the high flow velocities expected in the study area, an adaptive time-stepping scheme was employed to satisfy the Courant condition; Courant et al. (1967) parameter values were tuned through trial runs to span the range of feasible time steps for stable and accurate solutions. Model output intervals were set to 10 min for mapping layers, discharge hydrographs, and detailed profiles of water level and flow depth.

Model instabilities were initially observed, attributable to the complex topography (e.g., steep slopes, multiple hydraulic structures). Stability and efficiency were achieved by iteratively adjusting grid resolution, the solution scheme (e.g., dynamic wave), the Courant-based adaptive step parameters, and the ancillary time-step settings. The final configuration reduced computational cost/time while preserving hydraulically consistent results with sufficient accuracy.

To conclude this chapter, the subsequent figure provides a flowchart summarizing the proposed methodological framework (Figure 5).

3 Results

3.1 Hydrologic modeling/flow hydrographs

The outcomes of the rainfall-runoff model differ; for this application time series of parameters were utilized for each feature. Subsequently, a hydrologic simulation was performed, generating flow hydrographs for each subbasin and all points within the network; as depicted on the graphs below for the river basin outlet. For each scenario, flow hydrographs were introduced at key locations within each subbasin as deemed necessary during the execution of the LISFLOOD-FP hydraulic model. The flow hydrographs of each subbasin were extracted and stored in DSS format. The graphs depict the time variation of precipitation (design hyetographs) and discharge (flow hydrographs) at the catchment outlet under average antecedent soil moisture conditions (CN II) for 50, 100 and 1000-year return period, respectively (Figure 6). Based on the extracted flow hydrographs, the peak at the basin outlet was observed at 12 h and 10 min, where the greatest differences among the three scenarios occurred, with peak discharges of 218, 259.4, and 421.9 m^3/s for 50, 100, and 1000-year return period, respectively. The lag between the precipitation peak and the discharge peak was mostly attributed to simulated infiltration losses; since channel routing was assumed negligible.

3.2 Hydraulic modeling/flood hazard maps

To consider the issue of the inherent uncertainty in LISFLOOD, appearing in all water-cycle processes from small to large scales (Dimitriadis et al., 2021), a sensitivity analysis was performed to determine the error magnitude and range of all involved processes variability to flood risk (with the main primary processes to be rainfall and streamflow). Considering the low computational burden of the LISFLOOD-FP in combination with the capability of using small cell-sizes, as compared to the HEC-RAS 2D, where for the same cell-sizes the computational burden highly increased, we were able to perform a relatively semi-quantitative sensitivity analysis of the high-uncertainty parameters, such as the cell size (through the grid resolution), the topographic slopes of the channels and floodplain (through the river network configuration and condition in LISFLOOD-FP), and the rainfall-runoff magnitude (by varying the hydrograph time step), as shown in the Tables below. For each parameter combination, the computational load and maximum water depth were evaluated (Table 2), as these are the key indicators of the analytical performance we need to optimize for the setup of the HEC-RAS 2D model.

In Table 2, the results of the sensitivity analysis showcased that the maximum depth increased by 2 m, from 5.3 m to 7.3 m, when reducing the size of the cell. In Table 3, the probability of non-exceedance of depth for all flooded cells appeared to differ by approximately 10% between the different scenarios for depths of 0.5 m and 1 m, while for the depth of 2 m this difference decreases to 5% and for 5 m almost to 0%. Our analysis indicates that uncertainty associated with the above input-parameter variability, for all the return-periods and tested cell-sizes, varies from 5.7% to 2.7% for the 2 m depths and 21.2%–11.5%, showing small variation among scenarios for flood depths greater than 1 m, while the greatest flood-risk uncertainty occurs at depths of 1 m or less. This sensitivity analysis allowed the selection of 10 min for the hydrograph time-step. Also, a range between 25 m for the larger cell size at the floodplain area and 1-10, 3-10, 5–10 m for the smallest one at the river area is implemented in HEC-RAS 2D model, so that the topographic slopes are also more accurately preserved.

The outputs of LISFLOOD-FP confirmed the occurrence of severe flood inundation at the confluence of the Kalogiron stream and downstream along the Pikrodafni stream (Figure 1). The results also indicate flooding upstream of the Amphitheas and Poseidonos Avenue bridges—consistent with the documented 2013 flood event. Furthermore, the model highlighted extensive upstream flooding,

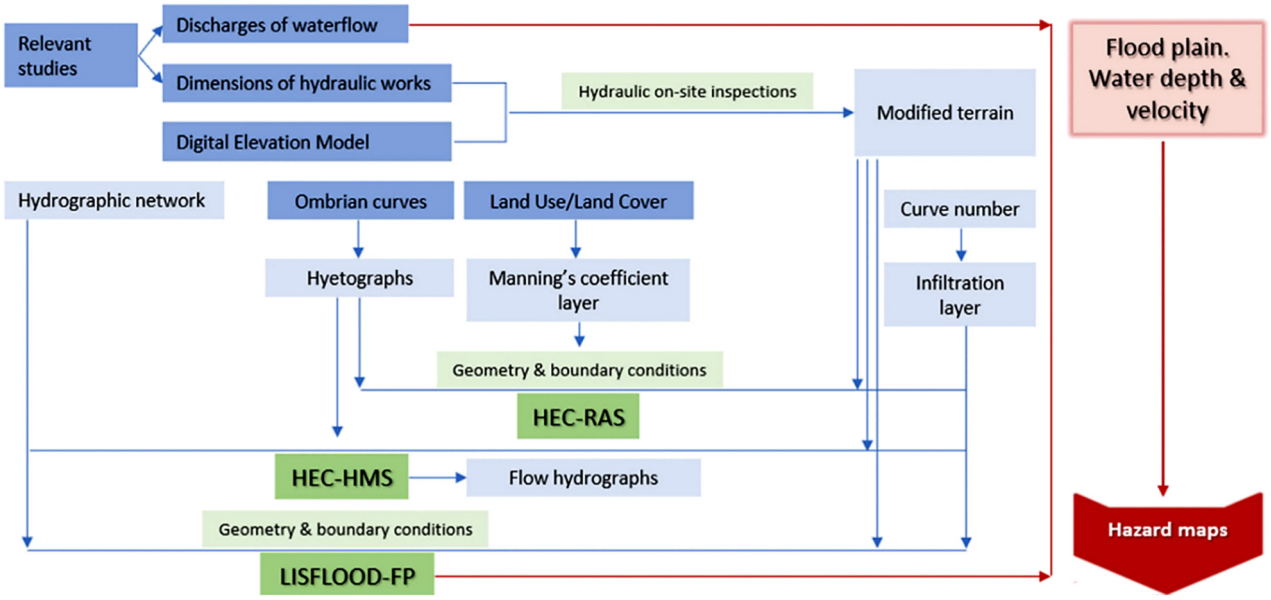

FIGURE 5
Flowchart of the applied methodology (Sargentis et al., 2025c).

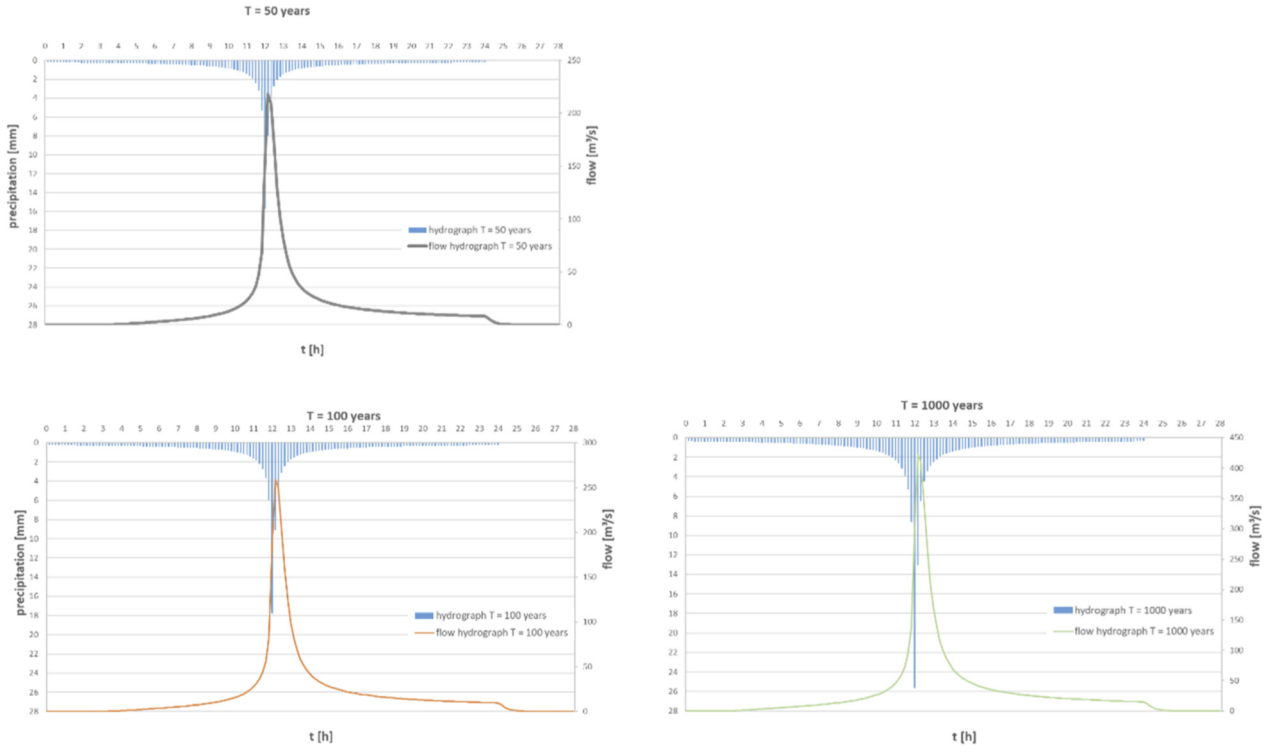

FIGURE 6
Hyetographs and hydrographs at a basin outlet under average antecedent soil moisture conditions (CN II) for 50, 100 and 1000-year return period scenarios.

underscoring the need for the implementation of flood-protection measures, as previously reported by the municipal Technical Services Directorate and confirmed through field inspections.

The results should be considered as underestimations of the actual flood response, since the LISFLOOD-FP model simulated fluvial flood, by applying the flow hydrographs in each subbasin.

TABLE 2 Flood inundation simulation scenarios using the LISFLOOD-FP hydraulic model.

Return period (years)	Grid size (m)	Flood hydrograph time step (min)	Channel configuration	Channel condition	Computational load (h)	Maximum water depth (m)
1000	20	10	Adverse	Adverse	0.5	5.3
1000	10	10	Adverse	Adverse	1.0	6.3
1000	5.6	10	Adverse	Adverse	2.0	6.8
50	5.6	10	Adverse	Adverse	2.0	6.8
100	5.6	10	Adverse	Adverse	2.0	6.8
1000	5.6	60	Adverse	Adverse	3.5	7.3
1000	5.6	60	Favourable	Favourable	3.5	5.7

TABLE 3 Exceedance probabilities of different flood depths for each flood inundation simulation scenario using the LISFLOOD-FP hydraulic model.

Return period (years)	Grid size (m)	Flood hydrograph time step (min)	Non-exceedance probability 0.5 m (%)	Non-exceedance probability 1 m (%)	Non-exceedance probability 2 m (%)	Non-exceedance probability 5 m (%)
1000	20	10	78.1	78.8	94.3	99.9
1000	10	10	80.7	81.6	95.6	99.8
1000	5.6	10	84.2	86.9	96.0	99.9
50	5.6	10	85.1	87.6	96.5	99.9
100	5.6	10	84.4	87.2	96.2	99.9
1000	5.6	60	84.3	86.0	96.7	99.9
1000	5.6	60	86.8	88.5	97.3	100.0

Rather than being used to directly calibrate the HEC-RAS, the LISFLOOD-FP was used as a supporting flexible model to assess parameter sensitivity and to perform consistency checks. In this way, it supported the computationally demanding two-dimensional (2D) HEC-RAS model, which applied the rain-on-grid methodology enhancing a more detailed representation of the flood dynamics.

The geospatial layers of flood inundation and velocity maps were produced by HEC-RAS model; thus, it is important to perform systematic post-processing in order to ensure the accuracy of the results. Geoprocessing operations created in Model Builder environment, run allowing the procedure to be repeated multiple times with different input datasets. This procedure enhanced the efficiency and the consistency of the results. A key step in the post-processing phase involved identifying and eliminating false water detections, particularly in sparse flooded areas located away from the river, which were likely artifacts of the modeling process. This was accomplished using an area threshold criterion (<300 m^2), ensuring that only significant and hydrologically relevant flood extents were retained. Conversely, small yet hydrologically meaningful flooded areas in close proximity to the river were preserved to maintain the accuracy of the flood extent delineation. The final mask generated through this process was systematically applied to both depth and velocity raster datasets, refining in order to eliminate scattered outliers and further smooth the flow locally, ensuring a more realistic and hydrodynamically coherent representation of the flood.

The outputs of the hydraulic simulation for each scenario were the flood inundation area, along with the spatial variation of flow depth and flow velocity for each time step. Maximum flow depth was extracted to derive flood hazard maps, where the maximum value at each cell needed to be estimated. The flood hazard maps for the examined scenarios, considering a 24-h rainfall duration, average antecedent soil moisture conditions (CN II), and 50, 100, and 1000 years return periods are presented below (Figure 7). Water levels were classified into five categories, as shown in the legend, and are represented with a gradation of blue shades from lower to higher hazard level in correspondence.

The 1000-year return period scenario has significant differences compared with the 50 and 100-year return period scenarios, since it constitutes the worst-case scenario. Specifically, the hydrodynamic simulations show that from the confluence of the Kalogiron stream with the Pikrodafni river and downstream (Figure 1), extensive flood phenomena occur. Mostly all the confluence of streams are overflowed locally even for the more frequent scenarios of 50 and 100-year return period.

The bridges at Amfitheas Street and Poseidonos Avenue fail even on the 50-year scenario, as occurred during the 2013 flood, with water inundating adjacent roads and residential areas.

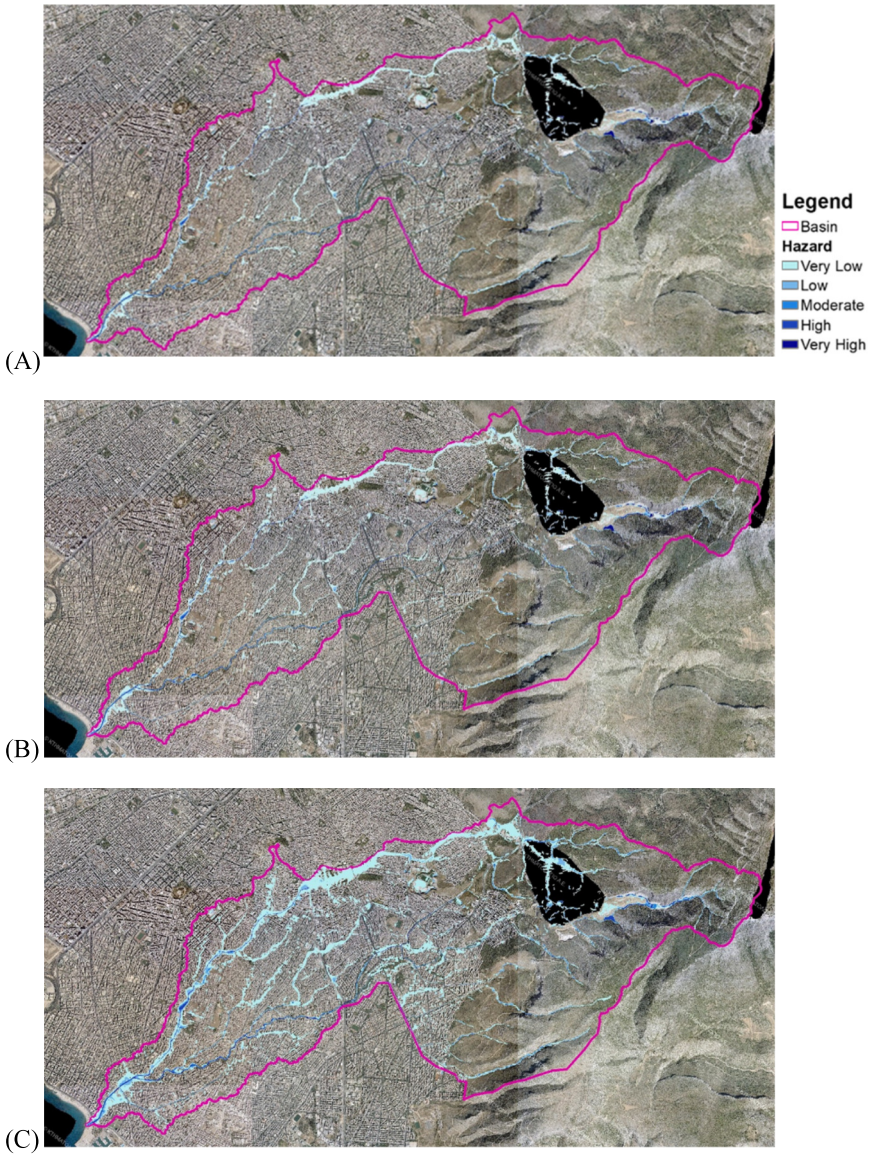

FIGURE 7
Flood Hazard maps of Pikrodafni river basin for 50 **(A)**, 100 **(B)** and 1000 **(C)** years return period scenarios.

Furthermore, it is observed that the areas discharging stormwater into the main stream through the stormwater drainage network also experience severe flooding, since they were designed to convey a 50-year flood. The results highlight that overflow is usually observed where there are hydro morphological alterations in the riverbeds, such as buried streams and sediment loads/trees that reduce the wetted cross section. An additional problem identified in the stormwater drainage pipes located at the upstream area, is the absence of inlet structures resulting in inadequate drainage of flows originating from the natural catchment. This problematic area was initially reported by the Technical Services Directorate of the relevant Municipality and verified through on-site inspections.

Thus, according to the flood risk, critical points were classified into three classes based on the priority level for taking measures. For the Pikrodafni river basin, 219 critical points were identified in 2022, while 79 points were classified as first priority and 50 and 90 were second and third priority critical points, respectively. Especially, for the first priority, the critical points were further classified according to their type, such as Buildings inside flood extent, Infrastructure inside flood extent and Residences with basements, as presented in the following map (Figure 8).

Generally, it is observed that many high-risk points were identified in residential areas, road networks and other critical infrastructure, such as schools and sports courts located in unstable riverbanks. The majority of first-priority critical points were identified as buildings and infrastructure located within the flood extent, with several positioned directly in the riverbed or on the stream banks. It was also observed that many areas exhibited illegal waste dumping and sediment deposits obstructing bridges and culverts, necessitating urgent clearance.

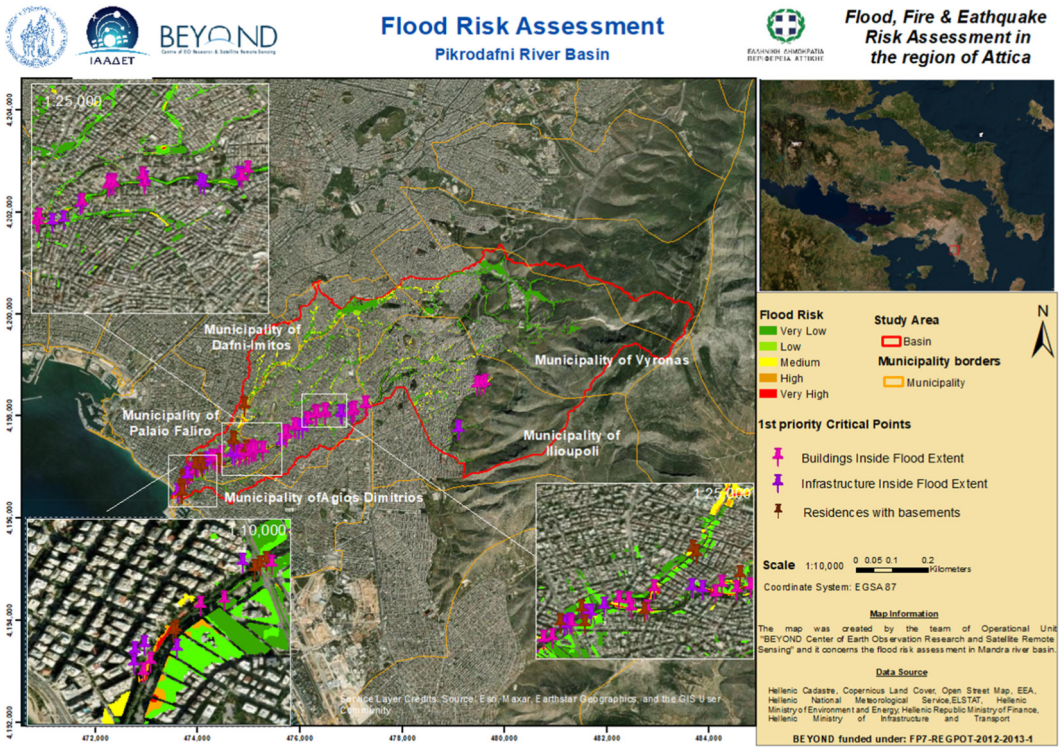

FIGURE 8
Flood Risk Map of Pikrodafni river basin including first priority critical points.

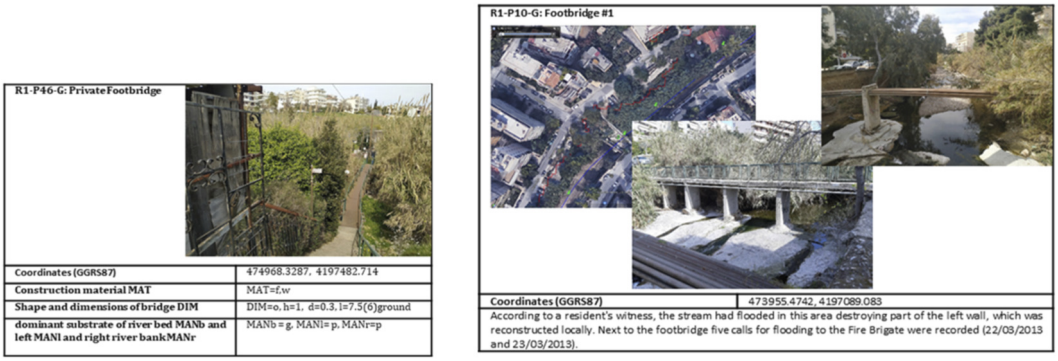

FIGURE 9
Technical reports for indicative critical points along the Pikrodafni river basin.

The delivery of critical points to the relevant authorities was crucial, since they constitute a recorded dataset depicting the current situation, which as was proposed, can be updated with the latest interventions, such as riverbed cleaning.

Also, for each critical point, a detailed technical report was delivered, including the basic characteristics/attributes based on the type of the critical point, with selected examples shown in the following Figure (Figure 9).

Pre-existing, collected and produced data were properly organized and stored on a user-friendly web platform, becoming available to all Prefecture's and Municipalities' services. The multi-risk GIS platform compiles ancillary datasets and outputs from flood, earthquake, and wildfire risk assessments, together with the corresponding technical reports, for the study areas in Attica.

4 Discussion

Flood assessment studies have also been conducted in the past, in the framework of Flood risk management plans of Directive 2007/60/EC analyzing different scenarios covering the Greek territory.

However, the outputs are not directly comparable due to methodological heterogeneity—differences in assumptions, input datasets, and spatial resolution—together with differing uncertainties (Dimitriadis et al., 2017).

Regarding the use of legacy spatial data, our attempt to integrate materials from older studies underscored three challenges: (i) the need for strong institutional communication with the responsible relevant authorities for the delivery of past studies; (ii) the necessity for a cross-methodological workflow that bridges desktop analysis and fieldwork to verify the accuracy of reported spatial and ancillary data; and (iii) the availability (or lack thereof) of GIS/CAD-editable formats in historical deliverables and its implications for requirements of data pre-processing. Accordingly, practical priorities for future work include readiness to combine diverse software tools and methods to consolidate legacy datasets into a single editable repository, proactive engagement with data-producing entities to obtain original editable files, and systematic validation via field campaigns and cross-study checks. These methodological insights are considered important because they can be generalized to other data-rich regions where historical information should be integrated into contemporary geospatial analyses for flood risk and related environmental assessments (Moraiti et al., 2024; Sargentis et al., 2024).

Field surveys were identified in this work as essential complements to flood-mitigation studies, providing ground-truth on site conditions, verifying compliance with design specifications, and capturing dynamic factors that affect infrastructure performance. On-site inspections reveal issues not evident remotely—by documenting as-built conditions—collecting useful information about infrastructure that might be missing from prior studies (such as the dimensions for accurate modeling) and identifying critical points across the river basin (Sargentis et al., 2025a; Sargentis et al., 2025b; Sargentis et al., 2025c). Also, field surveys enable quality control against flood-safety requirements and incorporate community knowledge, through communication with the public on-site.

Meanwhile, for the estimation of the rainfall intensity-duration-frequency (IDF) curve, an up-to-date, revised methodology for the study of IDF curves is developed and published, based on which the parameter values have been updated and spatially generalized across the entire Greek territory (Iliopoulou et al., 2024; Koutsoyiannis et al., 2024). This methodology provides the design rainfall parameters at 5 km × 5 km grid covering the entire Greek territory without the need to perform at-site estimations and sophisticated spatial interpolations, apart from a weighted parameter averaging over the study region (Koutsoyiannis et al., 2023). Therefore, new studies for the region are expected to benefit from a readily-available design rainfall parameterization for the study area.

More specifically, the regionalization of the parameters of the rainfall curves in the Greek Territory was based on the point estimates at the Water Division level that are obtained in the context of the contracts assigned for the first Revision of the Flood Risk Management Plans in application of the 2007 Directive/60/EC (European Parliament Council of the European Union, 2007). The regionalization aims to achieve a reliable model of rainfall curves with spatially varying parameters, with the finest possible spatial resolution, extending over the entire country. For this purpose, spatial interpolation methods with smoothing are utilized as well as newer, more reliable methodologies for spatial parameter estimation.

Also, the novelty of our study lies in the fact that the RoG approach was used since it is suitable for simulating compound pluvial-fluvial flooding, as observed in Pikrodafni river basin.

Regarding the use of different hydrodynamic models, Hankin et al. concluded that the growing versatility of various 2D hydrodynamic software packages played a crucial role in enabling the direct incorporation of lateral inflows and hydraulic structures into a 2D mesh, as well as allowing for flexible mesh creation around critical floodplain features such as embankments (Hankin et al., 2019). This was taken into consideration for the selection of these specific 2D hydraulic models, and was confirmed by the model results from our study.

Also, Mattas et al. performed sensitivity analysis for the model mesh size in the downstream area of Papadia dam, determining that the application of the densest 2D mesh increases the reliability of the model's results (Mattas et al., 2023), given the spatial resolution of the DEM. Another study also concluded that the increase of DEM spatial resolution leads to higher model accuracy, as indicated by the estimated accuracy indices (Pathan et al., 2022). However, the densest the mesh is, the more complex and time consuming the computations are (Pathan et al., 2022). Therefore, AI Pathan et al. recommend identifying a threshold for the DEM's spatial resolution to balance model accuracy with computational efficiency. Alexopoulos et al. also indicate the impact of DEM resolution on RoG model performance concluding that high-resolution DEMs (<1 m) are required for reliable RoG simulations (Alexopoulos et al., 2024). All the above analyses were considered during the mesh creation of our models, as a similar approach was adopted, taking into account the significance of each area within the computational mesh. To improve inundation modeling, particularly in areas with significant slope heterogeneity or special use, a terrain mosaic that integrates DTMs at multiple spatial resolutions is recommended. Zhou et al. achieved strong results using a drone-derived DTM within 2-D flood modeling of a mountainous urban basin in China (Zhou et al., 2025).

Model parameters should be calibrated using historical flood events within the area of interest in order to optimize the model and achieve high accuracy. The calibration strategy depends on the available ground-truth data type—e.g., stage or discharge from hydrometric/meteorological stations, *in-situ* water-depth measurements, or inundation extents derived from satellite or UAV (drone)/LiDAR imagery. In data-scarce or ungauged catchments where floods are detected remotely, integrating remote-sensing products with hydraulic/hydrologic modeling is an effective approach to estimate both the spatial extent and temporal evolution of events (Psomiadis et al., 2020; Konis et al., 2025). Consequently, simulating past floods enables robust model calibration, improving accuracy for flood-hazard assessments under alternative scenarios (Tansar et al., 2020) and for operational forecasting (Tran et al., 2020). In the Pikrodafni River basin, the most recent severe event in 2013 lacks sufficient observations for direct calibration. Thus, the availability of detailed data for calibration at different points of 2D models is a crucial factor for reliable model estimates (Merwade et al., 2008). Establishing a calibration framework anchored in available observations is considered fundamental for strengthening the overall methodology. Therefore, in terms of management plan it is proposed that future event-based models be

calibrated using the presented synthetic scenarios, herein, given their enhanced level of detail.

The recorded past 20 years - historic emergency calls related to flood events and were utilized to analyze and understand the dynamics of the flooding phenomenon in the study area. The data were collected mostly from the recorded Fire Brigade calls and other sources, such as media and technical studies (Tsergas, 2021). It was observed that except for the expected flooded areas, additional affected zones were identified, which were not represented in our results. This approach was implemented in the Vega Baja region in Spain for the September 2019 flood event (Ortiz et al., 2024), where the findings of this research highlight the critical role of incorporating emergency call data into flood management frameworks to strengthen preparedness, improve response, and build resilience in flood-prone areas. Additionally, this analysis could be further extended in order to improve the flood risk maps and achieve a more accurate mapping. Model calibration is essential for reliable flood simulation and hazard mapping.

In the framework of integrating modeling with uncertainty analysis and accuracy, Merwade et al. outlined the need for Probabilistic Flood Inundation Mapping, represented as surrounding zones outside the flood inundation, depending on the uncertainty of model parameters (Merwade et al., 2008). Applying probabilistic tools in flood inundation assessment and mapping is suggested as a good practice, since the representation of the results could be more understandable for stakeholders and improve the deterministic model framework, which additionally constrains the intrinsic limitations of the hydraulic models (Horritt and Bates, 2002; Neal et al., 2012; Dimitriadis et al., 2016).

Also, incorporating machine learning to physical models is widely used for flood prediction and involves the numerical simulations. However, there are many factors that need enhancements; indicating some representative examples below. High-resolution flood-probability maps are vital for risk assessment, yet their development is often constrained by limited historical data (Huang et al., 2025). The lack of historical flood event data which are utilized as training datasets, leads to the production of synthetic flood events providing flood depth data. Moreover, generating the simulated data required for probabilistic flood maps with physics-based models is computationally intensive and time-consuming, limiting practical feasibility (Huang et al., 2025). Huang et al. introduced the Precipitation-Flood Depth Generative Pipeline, a generative-ML–driven methodology that produces synthetic inundation data at a large scale and yields probabilistic flood maps through estimator methods. Another issue is that although machine-learning approaches to flood forecasting have advanced markedly, recent events reveal hydrologic responses that diverge from historical development trends (Qureshi et al., 2025). The failure to predict an extreme flood highlights the constraints of models trained primarily on past records, which struggle with out-of-distribution extremes. Strengthening robustness therefore requires richer datasets and novel methodological strategies. Next-Gen Group Method of Data Handling (Next-Gen GMDH), an innovative ML model was proposed using HEC-RAS simulations, for the creation of the synthetic training dataset of discharges, covering a wide range of potential flood events with up to 10,000 years return periods.

This study demonstrates that, while the individual hydrological and hydraulic models employed are well established, their integrated application within a unified, high-resolution framework constitutes a meaningful methodological advancement for urban flood-hazard assessment. The proposed workflow systematically combines design rainfall estimation, rainfall–runoff modeling, quasi-2D hydraulic simulations, and fully 2D rain-on-grid modeling, enabling the explicit representation of compound pluvial–fluvial flooding, which is a dominant but often insufficiently addressed process in densely urbanized basins.

A key contribution of the methodology lies in the terrain-based representation of both open and buried stream segments, derived from detailed field surveys and technical studies and incorporated directly into the DEM. This approach allows realistic enforcement of flow paths while preserving high spatial resolution, overcoming practical limitations associated with explicit culvert parameterization in large, complex urban models. In addition, the adoption of a dual-model strategy, whereby LISFLOOD-FP is used to explore parameter sensitivity and guide the configuration of the computationally demanding HEC-RAS 2D model, improves robustness and computational efficiency while enhancing confidence in model setup choices.

Further methodological advancement is provided through the development of an automated, database-driven mesh-generation and quality-control workflow, which reduces manual intervention, ensures geometric consistency, and enhances the transferability of the approach to other urban river basins. Beyond hazard mapping, the framework directly links modeling outputs to the identification and prioritization of critical flood-risk points at building-block scale, supporting risk-informed decision-making and operational flood management.

The methodology has also demonstrated its transferability and adaptability, through its successful application in different river basins, such as Garyllis river basin in Cyprus (Kountouri et al., 2024), where the same methodological workflow was implemented using the equivalent datasets derived from local or open access sources. Therefore, the methodology is transferable in terms of workflow and analytical steps, assuming the availability of equivalent national, European, or open-access datasets.

Overall, the presented methodology moves beyond a site-specific application by offering a holistic, reproducible, and transferable framework for high-resolution urban flood-hazard assessment. Future work should focus on extending the framework toward probabilistic flood inundation mapping and further uncertainty quantification, thereby strengthening its applicability for strategic planning and resilience-building in data-rich but complex urban environments.

5 Conclusion

The results of our study in the Pikrofafni river basin showcase several factors that exacerbate flooding, considering the impact of its characteristics to the flow. Urban areas covering more than 50% of the river basin, together with the burnt areas and the lack of green spaces, increase the surface runoff significantly, since the hydrological losses due to infiltration are low. The majority of the substreams are buried, but the water eventually follows the topographic slopes causing damage to the river network and the adjacent areas where the old riverbed used to be, as indicated by the results of the hydraulic simulations. Also, the contribution of the urban drainage network is relatively minor, especially in low frequency flood scenarios, even if the buried

streams were simulated as open channels. Generally, it is concluded that the hydromorphological alterations of the riverbed and riverbanks may cause flooding instead of food protection, as verified by (Stefanidis et al., 2020), and thus nature-based solutions need to be proposed.

Potential blockages on culverts/bridges and absence of inlet structures on the upstream technical works complicate the flow and cause local overflow, as have been identified in past events. Therefore, such locations were recorded as high priority critical points. The authorities responsible for such infrastructure were thus directed to take periodic actions for riverbed monitoring and cleaning, periodically. Additionally, the majority of high-risk areas identified in this research, were related to buildings that were constructed either on or very close to stream beds. Moreover, infrastructure such as sports courts, protective walls, perimeter fences for schools and properties were also identified on the stream's banks, highlighting the damages mostly due to erosion and requiring emergent intervention.

The outputs of each methodological stage were confirmed, evaluated and finalized based on stakeholders' feedback. It is the first time that such a holistic approach for flood risk assessment was implemented on a building block level in Greece. Also, the development of a web platform provided added value for support of operational response during crisis, preparedness planning, and strategic decision-making.

The prototype knowledge created through the project supports the Prefecture of Attica in the optimum implementation of the National Civil Protection Plan and the work of Civil Protection Coordination Bodies. Strategic design should be considered as an organized and planned response to the flood risk, with specific actions (prioritized works and measures), according to the responsibilities of each competent authority.

Data availability statement

The datasets presented in this study can be found in online repositories. The names of the repository/repositories and accession number(s) can be found in the article/Supplementary Material.

Author contributions

SS: Conceptualization, Data curation, Formal Analysis, Investigation, Methodology, Project administration, Resources, Software, Supervision, Validation, Visualization, Writing – original draft, Writing – review and editing. PD: Conceptualization, Formal Analysis, Investigation, Methodology, Resources, Software, Supervision, Validation, Writing – original draft, Writing – review and editing. VP: Writing – original draft, Writing – review and editing. AT: Conceptualization, Formal Analysis, Investigation, Methodology, Project administration, Resources, Supervision, Visualization, Writing – original draft, Writing – review and editing. TI: Writing – original draft, Writing – review and editing. G-FS: Writing – original draft, Writing – review and editing. RI: Writing – original draft, Writing – review and editing. DD: Writing – original draft, Writing – review and editing. EC: Writing – original draft. NM: Writing – review and editing. DK: Writing – review and editing. CK: Conceptualization, Formal Analysis, Funding acquisition, Resources, Supervision, Visualization, Writing – review and editing.

Funding

The author(s) declared that financial support was received for this work and/or its publication. Specifically, the research study was funded by the Region of Attica within the framework of the Programming Agreement «Earthquake, fire and flood risk assessment in the Region of Attica» (Part A) signed in March 2021 between the Prefecture of Attica and the National Observatory of Athens, as well as by the UNICORN project which has received funding from the European Union's Horizon Europe research and innovation programme under grant agreement No 101180172.

Acknowledgements

The author(s) would like to thank the Prefecture of Attica and the technical departments of the municipalities comprising the Pikrodafni River Basin for project support and correspondence for providing access to datasets and technical reports.

Conflict of interest

Author AT was employed by Edge in Earth Observation Sciences.

The remaining author(s) declared that this work was conducted in the absence of any commercial or financial relationships that could be construed as a potential conflict of interest.

Generative AI statement

The author(s) declared that generative AI was not used in the creation of this manuscript.

Any alternative text (alt text) provided alongside figures in this article has been generated by Frontiers with the support of artificial intelligence and reasonable efforts have been made to ensure accuracy, including review by the authors wherever possible. If you identify any issues, please contact us.

Publisher's note

Supplementary material

The Supplementary Material for this article can be found online at: https://www.frontiersin.org/articles/10.3389/fbuil.2026.1768439/full#supplementary-material

References

Alexopoulos, M. J., Dimitriadis, P., Iliopoulou, T., Bezak, N., Kobold, M., and Koutsoyiannis, D. (2024). Effects of digital elevation model resolution on rain-on-grid simulations: a case study in a Slovenian watershed. *Hydrological Sci. J.* 69, 1468–1485. doi:10.1080/02626667.2024.2378487

Anagnostopoulos, D., and Co, L. P. (2018). Delineation study of the pikrodafni stream from Sarantaporou Street to the river mouth. Athens: prefecture of Attica.

Bates, P. D., and De Roo, A. P. J. (2000). A simple raster-based model for flood inundation simulation. *J. Hydrology* 236, 54–77. doi:10.1016/S0022-1694(00)00278-X

Bates, P., Trigg, M., Neal, J., and Dabrowa, A. (2013). *LISFLOOD-FP user manual (code release 5.9.6)*. Bristol, United Kingdom: School of Geographical Sciences, University of Bristol.

Bellos, V., and Tsakiris, G. (2015). Comparing various methods of building representation for 2D flood modelling in Built-Up areas. *Water Resour. Manag.* 29, 379–397. doi:10.1007/s11269-014-0702-3

Beretta, R., Ravazzani, G., Maiorano, C., and Mancini, M. (2018). Simulating the influence of buildings on flood inundation in urban areas. *Geosciences* 8, 77. doi:10.3390/geosciences8020077

Centre for Research on the Epidemiology of Disasters (CRED) (2025). 2024 disasters in numbers. Brussels, Belgium: CRED (Centre for research on the epidemiology of disasters), UCLouvain. Available online at: https://files.emdat.be/reports/2024_EMDAT_report.pdf (Accessed December 5, 2025).

Chow, V. T. (1959). *Open-Channel hydraulics*. New York: McGraw-Hill, Inc.

Chow, V. T., Maidment, D. R., and Mays, L. W. (1988). *Applied hydrology*. International Edition. New York: McGraw-Hill Book Company.

Cook, A., and Merwade, V. (2009). Effect of topographic data, geometric configuration and modeling approach on flood inundation mapping. *J. Hydrology* 377, 131–142. doi:10.1016/j.jhydrol.2009.08.015

Courant, R., Friedrichs, K., and Lewy, H. (1967). On the partial difference equations of mathematical physics. *IBM J. Res. Dev.* 11, 215–234. doi:10.1147/rd.112.0215

de Moel, H., van Alphen, J., and Aerts, J. C. J. H. (2009). Flood maps in Europe – methods, availability and use. *Nat. Hazards Earth Syst. Sci.* 9, 289–301. doi:10.5194/nhess-9-289-2009

Diakakis, M., Andreadakis, E., Nikolopoulos, E. I., Spyrou, N. I., Gogou, M. E., Deligiannakis, G., et al. (2019). An integrated approach of ground and aerial observations in flash flood disaster investigations. The case of the 2017 Mandra flash flood in Greece. *Int. J. Disaster Risk Reduct.* 33, 290–309. doi:10.1016/j.ijdrr.2018.10.015

Dimitriadis, P., Tegos, A., Oikonomou, A., Pagana, V., Koukouvinos, A., Mamassis, N., et al. (2016). Comparative evaluation of 1D and quasi-2D hydraulic models based on benchmark and real-world applications for uncertainty assessment in flood mapping. *J. Hydrology* 534, 478–492. doi:10.1016/j.jhydrol.2016.01.020

Dimitriadis, P., Tegos, A., Petsiou, A., Pagana, V., Apostolopoulos, I., Vassilopoulos, E., et al. (2017). Flood Directive implementation in Greece: experiences and future improvements. *10th World Congr. Water Resour. Environ. "Panta Rhei* 57, 39–40.

Dimitriadis, P., Koutsoyiannis, D., Iliopoulou, T., Papanicolaou, P., Dimitriadis, P., Koutsoyiannis, D., et al. (2021). A global-scale investigation of stochastic similarities in marginal distribution and dependence structure of key hydrological-cycle processes. *Hydrology* 8, 59. doi:10.3390/hydrology8020059

Ennouini, W., Fenocchi, A., Petaccia, G., Persi, E., and Sibilla, S. (2024). A complete methodology to assess hydraulic risk in small ungauged catchments based on HEC-RAS 2D rain-on-grid simulations. *Nat. Hazards* 120, 7381–7409. doi:10.1007/s11069-024-06515-2

European Environment Agency (EEA) (2021). Urban Atlas Land Cover/Land Use 2018 (vector), Europe, 6-yearly. *Copernic. Land Monit. Serv. (CLMS) – Urban Atlas*. doi:10.2909/fb4dffa1-6ceb-4cc0-8372-1ed354c285e6

European Parliament; Council of the European Union (2007). Directive 2007/60/EC of the European Parliament and of the Council of 23 October 2007 on the assessment and management of flood risks. Available online at: https://eur-lex.europa.eu/legal-content/EN/TXT/?uri=CELEX:32007L0060 (Accessed March 25, 2021).

Giandotti, M. (1934). *Previsione delle piene e delle magre dei corsi d'acqua*. Roma: servizio Idrografico Italiano; Istituto Poligrafico dello Stato. Available online at: https://opac.sbn.it/ (Accessed June 5, 2021).

Guan, X., Vorogushyn, S., Apel, H., and Merz, B. (2023). Assessing compound pluvial-fluvial flooding: research status and ways forward. *Water Secur.* 19, 100136. doi:10.1016/j.wasec.2023.100136

Hankin, B., Metcalfe, P., Beven, K., and Chappell, N. A. (2019). Integration of hillslope hydrology and 2D hydraulic modelling for natural flood management. *Hydrology Res.* 50, 1535–1548. doi:10.2166/nh.2019.150

Hellenic Statistical Authority (2021). 2021 population-housing census. Available online at: https://www.statistics.gr/2021-census-pop-hous (Accessed November 18, 2022).

Horritt, M. S., and Bates, P. D. (2002). Evaluation of 1D and 2D numerical models for predicting river flood inundation. *J. Hydrology* 268, 87–99. doi:10.1016/S0022-1694(02)00121-X

Huang, L., Antolini, F., Mostafavi, A., Blessing, R., Garcia, M., and Brody, S. D. (2025). High-Resolution flood probability mapping using generative machine learning with large-scale synthetic precipitation and inundation data. *arXiv Preprint arXiv: 2409.13936*. Available online at: https://arxiv.org/abs/2409.13936 (Accessed December 15, 2025).

Iliopoulou, T., and Koutsoyiannis, D. (2022). "A parsimonious approach for regional design rainfall estimation: the case Study of Athens," in Proceedings of the 7th IAHR Europe Congress, *(Athens)*, 7–9. Available online at: http://www.iahr.org/library/infor?pid=22228 (Accessed May 5, 2023).

Iliopoulou, T., Koutsoyiannis, D., Malamos, N., Koukouvinos, A., Dimitriadis, P., Mamassis, N., et al. (2024). A stochastic framework for rainfall intensity–time scale–return period relationships. Part II: point modelling and regionalization over Greece. *Hydrological Sci. J.* 69, 1092–1112. doi:10.1080/02626667.2024.2345814

Kirpich, Z. P. (1940). Time of concentration of small agricultural watersheds. *Civ. Engineering* 10, 362.

Konis, A., Pagana, V., Sigourou, S., Tsouni, A., Salas, E., Tsoutsos, M.-C., et al. (2025). Integration of Remote Sensing and Hydraulic Modeling for Dynamic Flood Monitoring: a Copernicus Emergency Management Service for retrospective flood temporal analysis in Saarland, Germany. *Copernic. Meet.* doi:10.5194/egusphere-egu25-18097

Koukouvinos, A. (2014). Proposed methodological framework for the hydrology of the floods. Available online at: https://www.itia.ntua.gr/el/getfile/1468/1/documents/Presentation_Flood_Specifications.pdf (Accessed February 10, 2020).

Kountouri, J., Panagiotou, C. F., Tsouni, A., Sigourou, S., Pagana, V., Loulli, E., et al. (2024). "Flood hazard assessment and vulnerability analysis in Garyllis River Basin, Cyprus," in *Igarss 2024 - 2024 IEEE international geoscience and remote sensing symposium*, 3194–3198. doi:10.1109/IGARSS53475.2024.10641237

Kourgialas, N. N., and Karatzas, G. P. (2013). A flood risk approach for Mediterranean agricultural areas. *Hydrol. Process.* 27, 515–524. doi:10.1002/hyp.9269

Koutsoyiannis, D., and Baloutsos, G. (2000). Analysis of a long record of annual maximum rainfall in Athens, Greece, and design rainfall inferences. *Nat. Hazards* 22, 29–48. doi:10.1023/A:1008001312219

Koutsoyiannis, D., and Xanthopoulos, T. (1999). *Engineering hydrology*. 3rd Edn. Athens. doi:10.13140/RG.2.1.4856.0888

Koutsoyiannis, D., Andreadakis, A., Mavrodimou, R., Christofides, A., Mamassis, N., Efstratiadis, A., et al. (2008). "National Programme for the Management and Protection of Water Resources: support on the compilation of the national programme for water resources management and preservation," in *Department of water resources and environmental engineering*. Athens: National Technical University of Athens. doi:10.13140/RG.2.2.25384.62727

Koutsoyiannis, D., Mamassis, N., Efstratiadis, A., Zarkadoulas, N., and Markonis, Y. (2012). "Floods in Greece. Chapter 12," in *Changes in Flood Risk in Europe* (Wallingford, United Kingdom: IAHS Press), 238–256. doi:10.1201/b12348-12

Koutsoyiannis, D., Iliopoulou, T., Koukouvinos, A., Malamos, N., Mamasis, N., Dimitriadis, P., et al. (2023). *Technical report: production of maps with the updated parameters of rainfall intensity–duration–frequency (IDF) curves at the national level (implementation of EU Directive 2007/60/EC in Greece)*. Athens, Greece: National Technical University of Athens. Available online at: http://www.itia.ntua.gr/el/docinfo/2273/ (Accessed September 23, 2025).

Koutsoyiannis, D., Iliopoulou, T., Koukouvinos, A., and Malamos, N. (2024). A stochastic framework for rainfall intensity–time scale–return period relationships. Part I: theory and estimation strategies. *Hydrological Sci. J.* 69, 1082–1091. doi:10.1080/02626667.2024.2345813

Kyriakouli, V. (2022). *Sensitivity analysis of parameters in hydrology behavior of a drainage basin after a fire - application in the area of the watershed of the stream Picrodafni*. Athens: Department of Water Resources and Environmental Engineering, School of Civil Engineering, National Technical University of Athens. Available online at: https://www.itia.ntua.gr/en/docinfo/2232/ (Accessed December 6, 2022).

Loukas, A. (2015). Methods of assessment the design floods. Available online at: http://delos.uth.gr/opendelos/player?rid=bcdcc231 (Accessed February 2, 2021).

Manning, R. (1891). On the flow of water in open channels and pipes. *Trans. Institution Civ. Eng. Irel.* 20, 161–207.

Mattas, C., Karpouzos, D., Georgiou, P., and Tsapanos, T. (2023). Two-Dimensional modelling for dam break analysis and flood hazard mapping: a case Study of Papadia dam, Northern Greece. *Water* 15, 994. doi:10.3390/w15050994

Merwade, V., Olivera, F., Arabi, M., and Edleman, S. (2008). Uncertainty in flood inundation mapping: current issues and future directions. *J. Hydrol. Eng.* 13, 608–620. doi:10.1061/(ASCE)1084-0699(2008)13:7(608)

Merz, B., Hall, J., Disse, M., and Schumann, A. (2010). Fluvial flood risk management in a changing world. *Nat. Hazards Earth Syst. Sci.* 10, 509–527. doi:10.5194/nhess-10-509-2010

Ministry of Environment and Energy (2023). Preliminary flood risk assessment | national overview – 2nd cycle: flood risk management plans. Ministry of

environment and energy. Available online at: https://floods.ypeka.gr/sdkp-lap/prelim-eval-2round/ (Accessed November 10, 2025).

Ministry of Environment and Energy (2025). First revision of the flood risk management plan for the Attica River Basin district (EL06). *Ministry Environ. Energy*. Available online at: https://floods.ypeka.gr/wp-content/uploads/2025/05/EL06_SDKP_1st_REV.pdf (Accessed November 17, 2025).

Moraiti, K., Sigourou, S., Dimitriadis, P., Ioannidis, R., Benekos, I., Iliopoulou, T., et al. (2024). Documenting the changing floodplain of Nileas Basin in north euboea (Greece) before and after storms daniel and elias. *Rural Regional Dev.* 2, 10013. doi:10.35534/rrd.2024.10013

Neal, J., Villanueva, I., Wright, N., Willis, T., Fewtrell, T., and Bates, P. (2012). How much physical complexity is needed to model flood inundation? *Hydrol. Process.* 26, 2264–2282. doi:10.1002/hyp.8339

Ortiz, G., Aznar-Crespo, P., Oliva, A., Olcina-Cantos, J., and Aledo, A. (2024). Uses and opportunities of emergency calls as a resource for flood risk management. *Int. J. Disaster Risk Reduct.* 100, 104160. doi:10.1016/j.ijdrr.2023.104160

Ourloglou, O., Stefanidis, K., and Dimitriou, E. (2020). Assessing nature-based and classical engineering solutions for flood-risk reduction in urban streams. *J. Ecol. Eng.* 21, 46–56. doi:10.12911/22998993/116349

Papaioannou, G., Vasiliades, L., Loukas, A., and Aronica, G. (2017). Probabilistic flood inundation mapping at ungauged streams due to roughness coefficient uncertainty in hydraulic modelling. *Adv. Geosciences* 44, 23–34. doi:10.5194/adgeo-44-23-2017

Pappenberger, F., Beven, K., Ms, H., and Blazkova, S. (2005). Uncertainty in the calibration of effective roughness parameters in HEC-RAS using inundation and downstream level observations. *J. Hydrology* 302, 46–69. doi:10.1016/j.jhydrol.2004.06.036

Partington, D., Thyer, M., Shanafield, M., McInerney, D., Westra, S., Maier, H., et al. (2022). Predicting wildfire induced changes to runoff: a review and synthesis of modeling approaches. *WIREs Water* 9, e1599. doi:10.1002/wat2.1599

Patel, K. P. (2009). *Watershed modeling using HEC-RAS, HEC-HMS, and GIS models: a case study of the Wreck Pond Brook Watershed in Monmouth County*. New Jersey: Rutgers University - Graduate School - New Brunswick. doi:10.7282/T31R6QQC

Pathan, A. I., Agnihotri, P. G., Patel, D., and Prieto, C. (2022). Mesh grid stability and its impact on flood inundation through (2D) hydrodynamic HEC-RAS model with special use of Big Data platform—a study on Purna River of Navsari city. *Arab. J. Geosci.* 15, 659. doi:10.1007/s12517-022-09813-w

Presidential Decree (1974). On the fees of engineers for the preparation of studies, supervision, acceptance, *etc*. of transportation, hydraulic and building works, as well as topographic, cadastral and cartographic works and related technical study specifications. Available online at: https://www.elinyae.gr/ethniki-nomothesia/pd-6961974-fek-301a-8101974?utm_source=chatgpt.com (Accessed December 5, 2025).

Psomiadis, E., Diakakis, M., and Soulis, K. X. (2020). Combining SAR and optical Earth observation with hydraulic simulation for flood mapping and impact assessment. *Remote Sens.* 12, 3980. doi:10.3390/rs12233980

Qureshi, M. U. A., Amiri, A., Ebtehaj, I., Guimere, S. J., Cunderlik, J., and Bonakdari, H. (2025). Coupling HEC-RAS and AI for River morphodynamics assessment under changing flow regimes: enhancing disaster preparedness for the Ottawa River. *Hydrology* 12, 25. doi:10.3390/hydrology12020025

Region of Thessaly (2020). "Summary report on the proposal for the delineation of the Malakassiotikos stream for the construction of a small hydroelectric power plant with a capacity of 3.6 MW at the location "Kokkini Petra,"," in *The local communities of Kalomira and Matoneri, in the municipal unit of Kastania, Municipality of Kalampaka, Regional Unit of Trikala*.

Residents (2025). Residents' questionnaire on infrastructure construction. Available online at: https://docs.google.com/forms/d/e/1FAIpQLSdI6QXyzkbhNviFov3O5EuErRQodgDnt23L6g4F618evXzpIA/viewform?usp=embed_facebook (Accessed March 5, 2026).

Rozos, E., Bellos, V., Kalogiros, J., Mazi, K., Rozos, E., Bellos, V., et al. (2023). Efficient flood early warning System for Data-Scarce, karstic, mountainous environments: a case Study. *Hydrology* 10, 203. doi:10.3390/hydrology10100203

Sajikumar, N., and Remya, R. S. (2015). Impact of land cover and land use change on runoff characteristics. *J. Environ. Manag.* 161, 460–468. doi:10.1016/j.jenvman.2014.12.041

Sargentis, G.-F., Moraiti, K., Benekos, I., Ioannidis, R., and Mamassis, N. (2024). Fast-Track documentation of the alterations on the landscape, before and after a natural Hazard—Case Study: north euboea Greece before and after storms daniel and elias. *Rural Regional Dev.* 2, 10016. doi:10.70322/rrd.2024.10016

Sargentis, G. F., Ioannidis, R., Kougkia, M., Benekos, I., Iliopoulou, T., Dimitriadis, P., et al. (2025a). "Do floods attack cities or cities invade flood plains? Case Study: athens, Greece," in *Proceedings of the international conferences on digital technology driven engineering 2024*. Editors N. D. Lagaros, R. Z. Alrousan, K. M. Abdalla, M. C. Phocas, and G. C. Marano (Cham: Springer Nature Switzerland), 216–224. doi:10.1007/978-3-031-92044-8_21

Sargentis, G. F., Ioannidis, R., Kougkia, M., Benekos, I., Iliopoulou, T., Dimitriadis, P., et al. (2025b). "The technological evolution in flood risk estimation," in *Proceedings of the international conferences on digital technology driven engineering 2024*. Editors N. D. Lagaros, R. Z. Alrousan, K. M. Abdalla, M. C. Phocas, and G. C. Marano (Cham: Springer Nature Switzerland), 225–235. doi:10.1007/978-3-031-92044-8_22

Sargentis, G.-F., Iliopoulou, T., Ioannidis, R., Kougkia, M., Benekos, I., Dimitriadis, P., et al. (2025c). Technological advances in flood risk assessment and related operational practices since the 1970s: a case Study in the pikrodafni River of Attica. *Water* 17, 112. doi:10.3390/w17010112

Siakara, G., Gourgouletis, N., and Baltas, E. (2024). Assessing the efficiency of fully two-dimensional hydraulic HEC-RAS models in Rivers of Cyprus. *Geographies* 4, 513–536. doi:10.3390/geographies4030028

Sigourou, S., Pagana, V., Dimitriadis, P., Tsouni, A., Iliopoulou, T., Sargentis, G.-F., et al. (2022a). "Flood risk assessment in the region of Attica," in 9th international conference on civil protection and new technologies - safe thessaloniki 2022, *(Thessaloniki, Greece)*. Available online at: http://www.itia.ntua.gr/en/docinfo/2238/ (Accessed April 7, 2023).

Sigourou, S., Pagana, V., Dimitriadis, P., Tsouni, A., Iliopoulou, T., Sargentis, G.-F., et al. (2022b). "Proposed methodology for urban flood-risk assessment at river-basin level: the case study of the Pikrodafni river basin in Athens, Greece," in *Global flood partnership 2022 annual meeting*. Available online at: http://www.itia.ntua.gr/en/docinfo/2237/ (Accessed April 9, 2023).

Sigourou, S., Tsouni, A., Pagana, V., Sargentis, G.-F., Dimitriadis, P., Ioannidis, R., et al. (2023). "An advanced methodology for field visits towards efficient flood management on building block level," in *European geosciences union general assembly 2023*. doi:10.5194/egusphere-egu23-16168

Stathakis, D. (2022). Crowdsourced and open data in the Hellenic Cadastre. Available online at: https://www.eurocadastre.org/pdf/2022/Czech2022eu/presentaciones/Session%203/5_GR%20_Crowdsourced%20and%20open%20data%20in%20the%20Hellenic%20cadastre%20.pdf?utm_source=chatgpt.com (Accessed March 5, 2026).

Stefanidis, K., Latsiou, A., Kouvarda, T., Lampou, A., Kalaitzakis, N., Gritzalis, K., et al. (2020). Disentangling the main components of hydromorphological modifications at reach Scale in Rivers of Greece. *Hydrology* 7, 22. doi:10.3390/hydrology7020022

Tansar, H., Babur, M., and Karnchanapaiboon, S. L. (2020). Flood inundation modeling and hazard assessment in Lower Ping River Basin using MIKE FLOOD. *Arab. J. Geosci.* 13, 934. doi:10.1007/s12517-020-05891-w

Tran, V. N., Dwelle, M. C., Sargsyan, K., Ivanov, V. Y., and Kim, J. (2020). A novel modeling framework for computationally efficient and accurate real-time ensemble flood forecasting with uncertainty quantification. *Water Resour. Res.* 56, e2019WR025727. doi:10.1029/2019WR025727

Tsergas, A. (2021). "Flood risk in Attica: recording and analysis of events using GIS,". Athens: National Technical University of Athens. doi:10.26240/heal.ntua.21499

Tsouni, A., Sigourou, S., Pagana, V., Tsoutsos, M.-C., Dimitriadis, P., Sargentis, G.-F., et al. (2025). Multi-Parameter flood risk assessment and management planning at high spatial resolution in the Region of Attica, Greece. *IEEE J. Sel. Top. Appl. Earth Observations Remote Sens.* 18, 1–12. doi:10.1109/JSTARS.2025.3613569

United Nations Office for Disaster Risk Reduction (UNDRR) (2015). Sendai framework for disaster risk reduction 2015–2030. Available online at: https://www.undrr.org/publication/sendai-framework-disaster-risk-reduction-2015-2030 (Accessed October 9, 2025).

U.S. Army Corps of Engineers (2020). HEC-RAS (Version 6.0). Available online at: https://www.hec.usace.army.mil/software/hec-ras/ (Accessed September 19, 2022).

U.S. Army Corps of Engineers, Hydrologic Engineering Center (2025). HEC-RAS 2D user's manual. Davis, CA: USACE hydrologic engineering Center. Available online at: https://www.hec.usace.army.mil/confluence/rasdocs/r2dum/latest (Accessed October 9, 2025).

U.S. Army Corps of Engineers, Hydrologic Engineering Center (2018). *HEC-HMS Hydrologic Modeling System User's Manual (Version 4.3)*. Davis, CA: U.S. Army Corps of Engineers.

Van Westen, C. J. (2013). "3.10 remote sensing and GIS for natural hazards assessment and disaster risk management,", 3. Elsevier, 259–298. doi:10.1016/B978-0-12-374739-6.00051-8

Varra, G., İnan, Ç. A., Della Morte, R., Tartaglia, M., Fiduccia, A., Zammuto, A., et al. (2025). Assessment of direct rainfall and flood-induced damage to land transport infrastructure using two-dimensional HEC-RAS 6.6 rain-on-grid simulations. *Nat. Hazards* 121, 17615–17645. doi:10.1007/s11069-025-07484-w

Wang, N., Sun, F., Koutsoyiannis, D., Iliopoulou, T., Wang, T., Wang, H., et al. (2023). How can changes in the human–flood distance mitigate flood fatalities and displacements? *Geophys. Res. Lett.* 50, e2023GL105064. doi:10.1029/2023GL105064

Wannous, C., and Velasquez, G. (2017). United Nations Office for Disaster Risk Reduction (UNISDR)—Unisdr's contribution to science and technology for Disaster Risk Reduction and the role of the international consortium on Landslides (ICL)., in *Advancing culture of living with landslides*, eds. K. Sassa, M. Mikoš, and Y. Yin Ljubljana: Springer International Publishing, 109–115. doi:10.1007/978-3-319-59469-9_6

Wing, O. E. J., Bates, P. D., Quinn, N. D., Savage, J. T. S., Uhe, P. F., Cooper, A., et al. (2024). A 30 m global flood inundation model for any climate scenario. *Water Resour. Res.* 60, e2023WR036460. doi:10.1029/2023WR036460

Woodward, D., Hawkins, R., Jiang, R., Hjelmfelt, A., Mullem, J., and Quan, Q. (2003). Runoff curve number method: examination of the initial abstraction ratio. 10. 1, 10. doi:10.1061/40685(2003)308

Wyżga, B., Kundzewicz, Z. W., Konieczny, R., Piniewski, M., Zawiejska, J., and Radecki-Pawlik, A. (2018). Comprehensive approach to the reduction of river flood risk: case study of the Upper Vistula Basin. *Sci. Total Environ.* 631 (632), 1251–1267. doi:10.1016/j.scitotenv.2018.03.015

Yan, H., Gao, Y., Wilby, R., Yu, D., Wright, N., Yin, J., et al. (2024). Urbanization further intensifies short-duration rainfall extremes in a warmer climate. *Geophys. Res. Lett.* 51, e2024GL108565. doi:10.1029/2024GL108565

Zábori, J., Betterle, A., Corzo, T. M., D'angelo, C., Garcia, P. M., Lemke, C.-D., et al. (2024). European Flood Awareness System – a technical assessment of CEMS EFAS performance during the floods in Northern Germany in December 2023/January 2024. *JRC Publ. Repos.* doi:10.2760/1959574

Zhou, X., Mou, L., Ao, T., Huang, X., and Yang, H. (2025). Effect of the spatial resolution of digital terrain data obtained by drone on urban fluvial flood modeling of mountainous regions. *Hydrology Earth Syst. Sci.* 29, 1963–1980. doi:10.5194/hess-29-1963-2025